LASER INTERFEROMETER GRAVITATIONAL WAVE OBSERVATORY

LIGO Laboratory / LIGO Scientific Collaboration

LIGO-T0900453-v2 *LIGO* 3/10/10

ETM-Telescope

Comparison of Off-axis Parabolic Telescope with Spherical Mirror Secondary, or Triplet Lens

Michael Smith

Distribution of this document:
LIGO Scientific Collaboration

This is an internal working note
of the LIGO Laboratory.

California Institute of Technology
LIGO Project – MS 18-34
1200 E. California Blvd.
Pasadena, CA 91125
Phone (626) 395-2129
Fax (626) 304-9834
E-mail: info@ligo.caltech.edu

Massachusetts Institute of Technology
LIGO Project – NW22-295
185 Albany St
Cambridge, MA 02139
Phone (617) 253-4824
Fax (617) 253-7014
E-mail: info@ligo.mit.edu

LIGO Hanford Observatory
P.O. Box 1970
Mail Stop S9-02
Richland WA 99352
Phone 509-372-8106
Fax 509-372-8137

LIGO Livingston Observatory
P.O. Box 940
Livingston, LA 70754
Phone 225-686-3100
Fax 225-686-7189

http://www.ligo.caltech.edu/

Table of Contents

Figures

Tables

Abstract

The purpose of this technical note is to describe the ellipticity and wavefront distortion of a parabolic telescope and a hybrid ETM Telescope, comprised of an off-axis parabolic primary mirror and a 1) spherical secondary mirror, or 2) triplet lens secondary. The telescope is part of the Transmon System for aLIGO.

1 Introduction

The purpose of this technical note is to describe the ellipticity and wavefront distortion of a hybrid ETM Telescope, comprised of an off-axis parabolic primary mirror and a 1) spherical secondary mirror, or 2) triplet lens secondary.

2 Physical Layout of the ETM Telescope

A preliminary design layout of the Transmon System with the ETM Telescope placed below the Transmon optical table, is shown in Figure 3. Various designs are considered for the ETM Telescope.

2.1 Off-axis Parabolic Design

Off-axis parabolic mirrors form a reflective telescope, as shown in Figure 1. The ZEMAX layout is rotated 180 degrees from the actual position in the Transmon System. The primary focal length is 2000 mm, and the secondary focal length is 66.7 mm. The input aperture is 190 mm, and the telescope has a speed of f/11. The on-axis beam and the -1.8 deg off-axis Hartmann beam are shown.

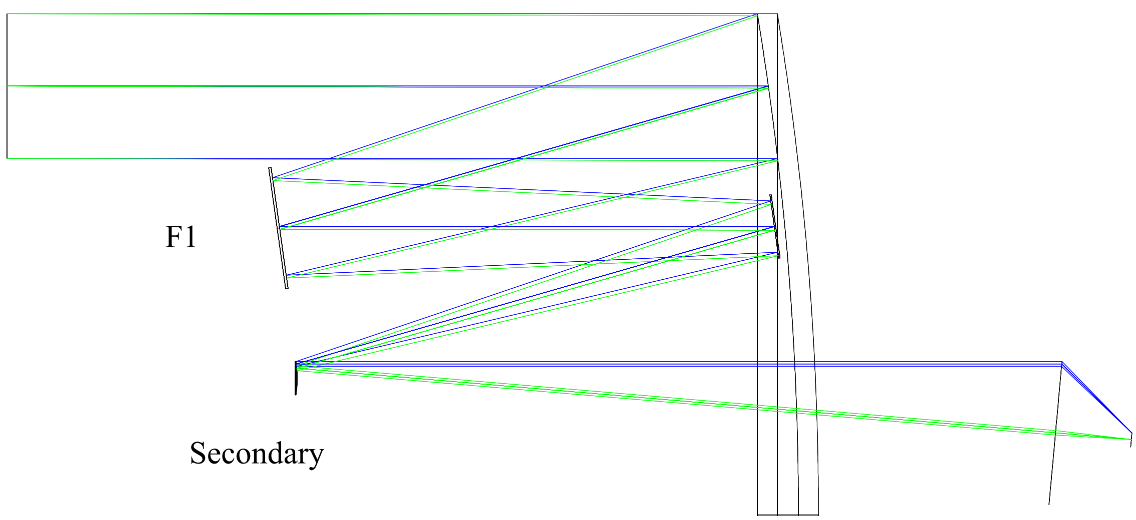

Figure 1: ZEMAX Sequential Model, Off-axis Parabolic

2.2 Hybrid Parabolic/Spherical Mirror Design

The hybrid design of the ETM Telescope will retain the off-axis parabolic primary mirror, but will use a spherical secondary mirror, as shown in Figure 2. The spacing between the first fold mirror, F1, and the secondary mirror will be reduced to the smallest practical distance of approximately 5.5 in. (140 mm).

The spherical secondary mirror will be steered in the vertical plane to minimize the angle of incidence on the secondary mirror. The practical minimum incident angle is 4.3 degrees at the surface of the secondary mirror.

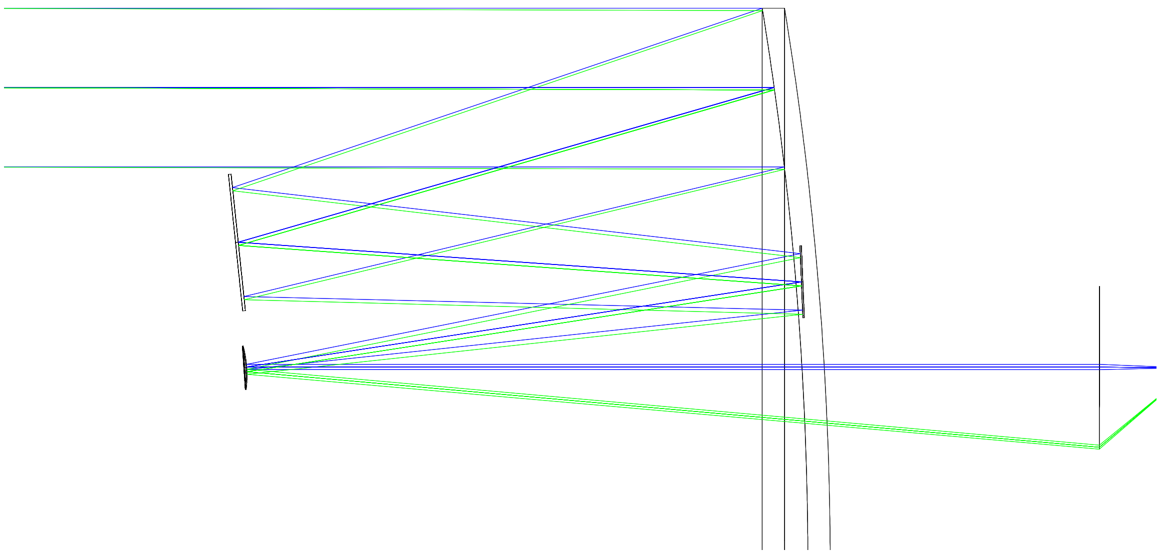

Figure 2: ZEMAX Sequential Model, 4.3 Deg Incidence Angle

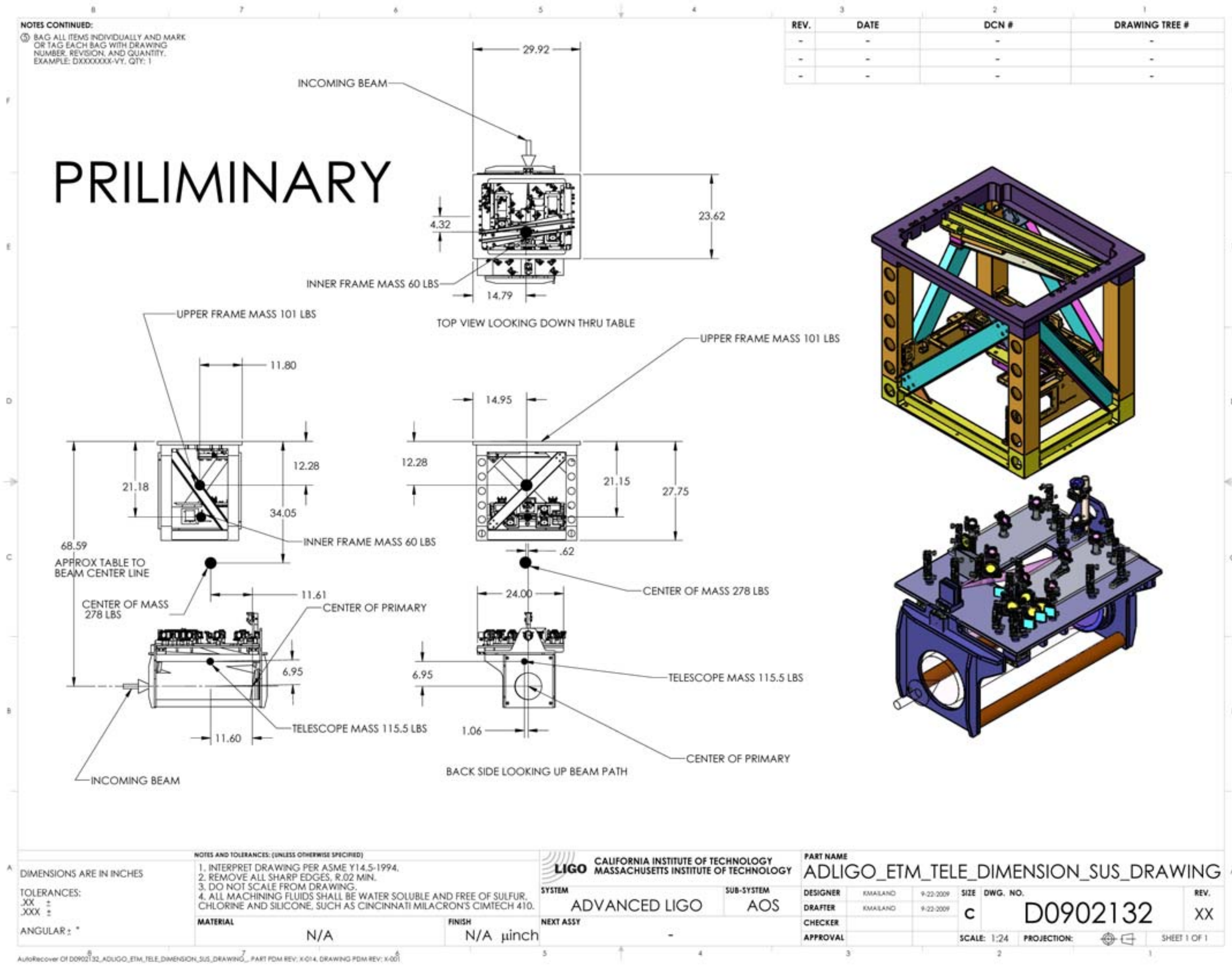

Figure 3: ETM Telescope/Transmon with Suspension

2.3 Hybrid: Parabolic Mirror Primary with Triplet Lens Secondary

The hybrid design of the ETM Telescope will retain the off-axis parabolic primary mirror, but will use a triplet achromatic lens for the secondary element. A third fold mirror will be placed at the approximate location of the prior spherical mirror. The entire telescope assembly will be placed beneath the Transmon optical table.

In order to accommodate the 0.532nm Hartman reference beam, the clear aperture of the triplet lens must be > 25mm. A commercially available triplet lens with a 25mm clear aperture was chosen. The effective focal length is 125mm—this results in a magnification of 16 rather than the original design value of 30.0. The 1064nm beam is aligned on the axis of the triplet lens; the 0.532nm Hartmann beam is displaced from the optical axis by approximately 6mm, as shown in Figure 4.

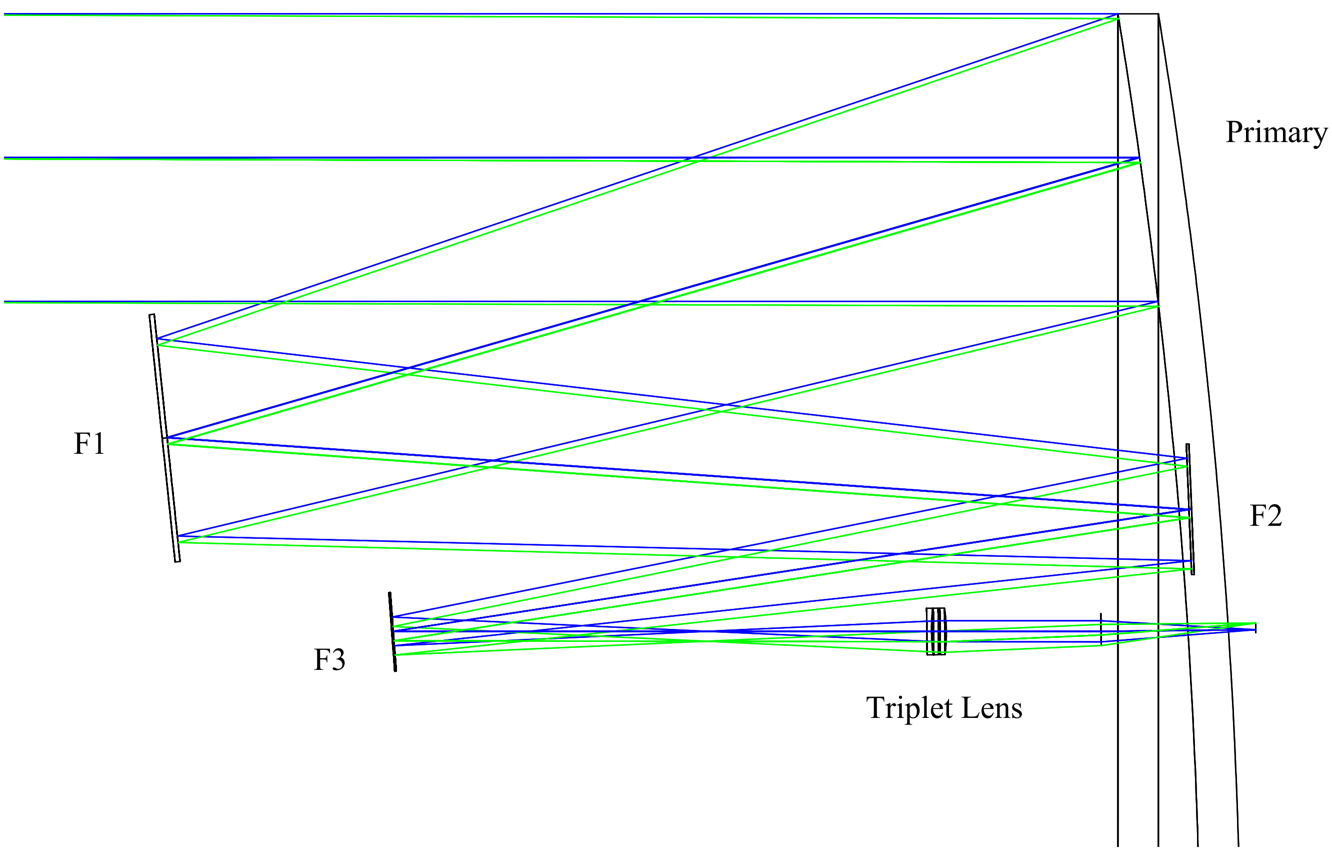

Figure 4: ZEMAX Sequential Model, Off-axis Parabolic Primary with Triplet lens Secondary

3 Telescope Performance

The telescope was focused to obtain the smallest output spot at the focal plane of a paraxial 100mm EFL lens. This places the output beam waist approximately at the output of the telescope.

The wavefront function was calculated by the ZEMAX wavefront map analysis program.

The contour of the output beam was calculated using the Physical Optics Propagation program with an input beam waist of 11.5 mm located 2000 m in front of the telescope primary mirror.

The spot diagram is produced in ZEMAX by tracing rays and measuring the geometric spot size in the vicinity of the focal plane of the 100mm EFL paraxial lens. The black circle in the diagram is the Airy disc, which represents the diffraction spot size. The Rayleigh range can be estimated as the distance away from the focus where the geometric spot is equal to the Airy disc diameter.

3.1 Parabolic Telescope

3.1.1 Output Beam Contour

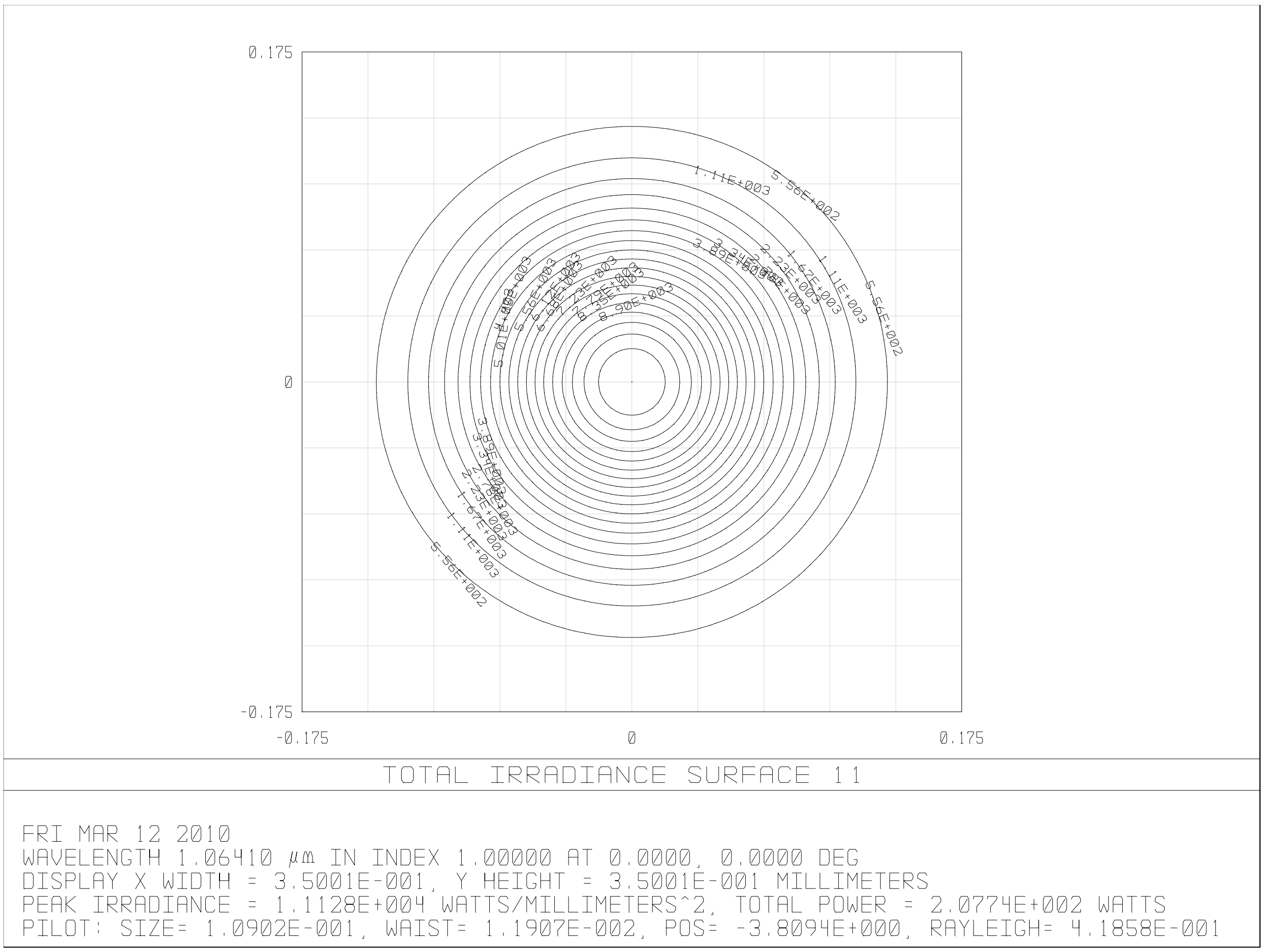

Figure 5: Physical Optics Output Beam Contour, Parabolic Telescope

The beam ellipticity was calculated by taking the ratio of the x and y widths of the beam contour.

3.1.2 Spot Diagram

The parabolic telescope exhibits negligible astigmatism on axis, and also with a -0.18 deg tilt of the input beam in the plane of the telescope.

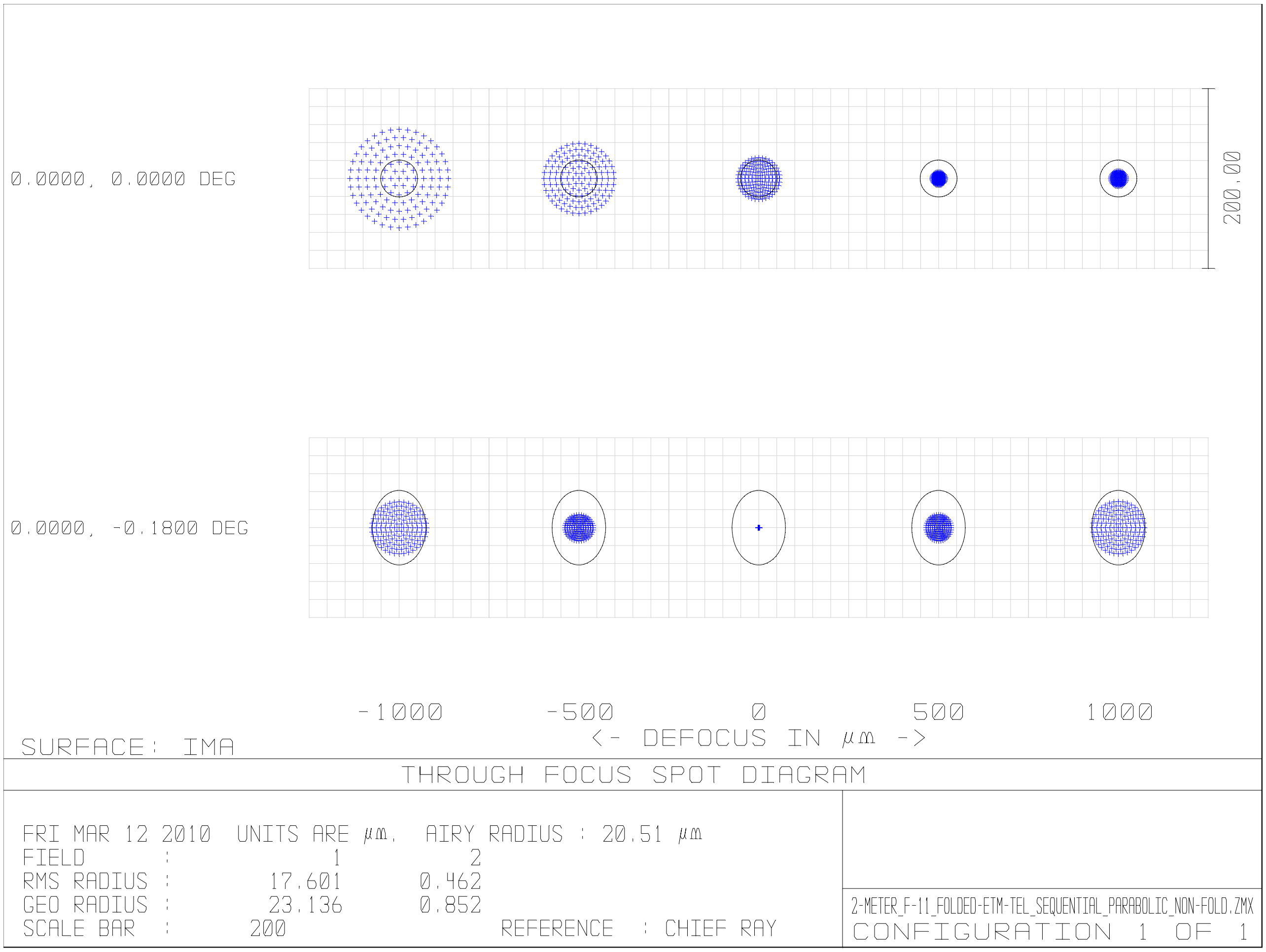

Figure 6: Spot Diagrams through Focus for 0 deg Field and -0.18 deg Field, Parabolic Telescope Case

3.1.3 Wavefront Aberration

The parabolic telescope exhibits diffraction limited performance on-axis and at the -0.18 deg field angle.

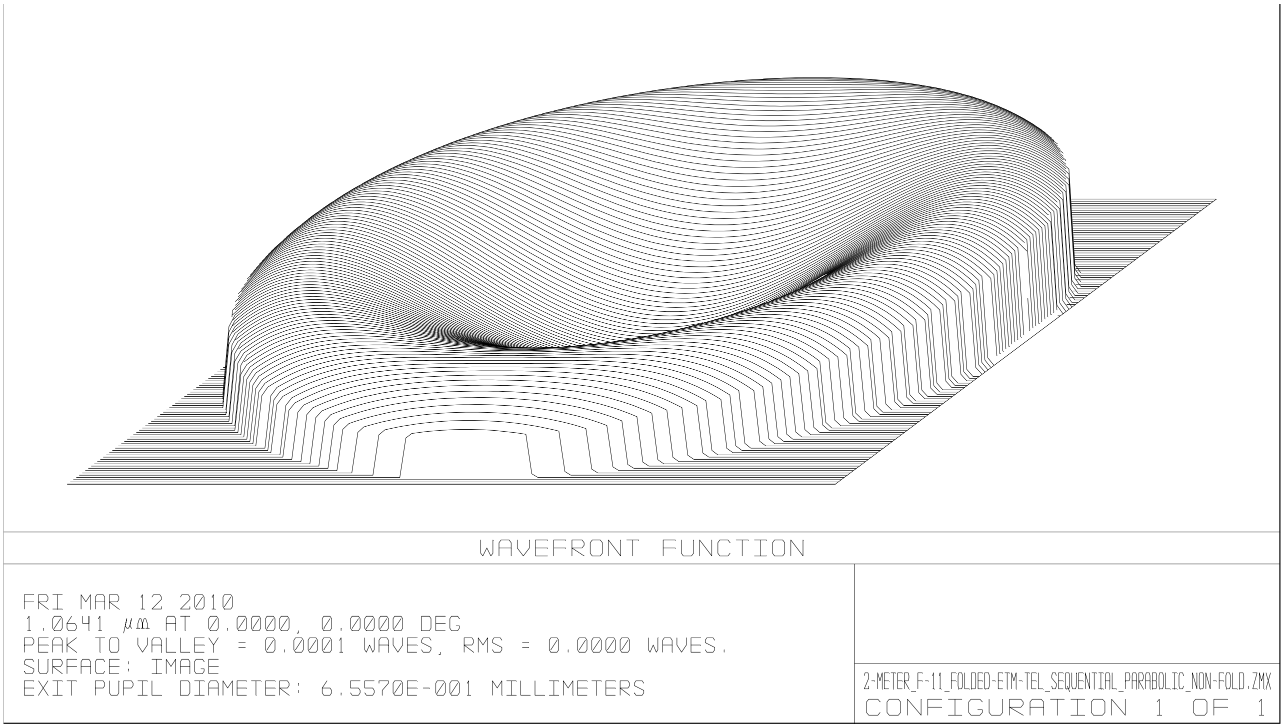

Figure 7: Wavefront Aberration on-axis, Parabolic Telescope

3.1.4 Parabolic Telescope Case: Effect of Telescope Tilt

The parabolic telescope retains diffraction-limited performance over the entire range of tilt angles.

Table 1: Ellipticity and Aberration vs Telescope Tilt, Parabolic Telescope

Telescope Tilt, Deg	**Ellipticity**	**Aberration, waves peak to valley**
0	1.000	0.0001
-0.05	1.005	0.0228
-0.1	1.05	0.0842
-0.18	1.04	0.2249
0.1	1.07	0.0830
0.18	1.08	0.2245

3.2 Parabolic Primary with Spherical Secondary

The following analysis was made with a range of incidence angles at the secondary spherical mirror from 3.9 deg to 6.1 deg, and a wavelength of 1064 nm.

3.2.1 Incidence Angle 3.9 Deg.

This is the smallest incidence angle that is practical with the physical constraints of the ETM Telescope/Transmon table.

3.2.1.1 ZEMAX Sequential Model

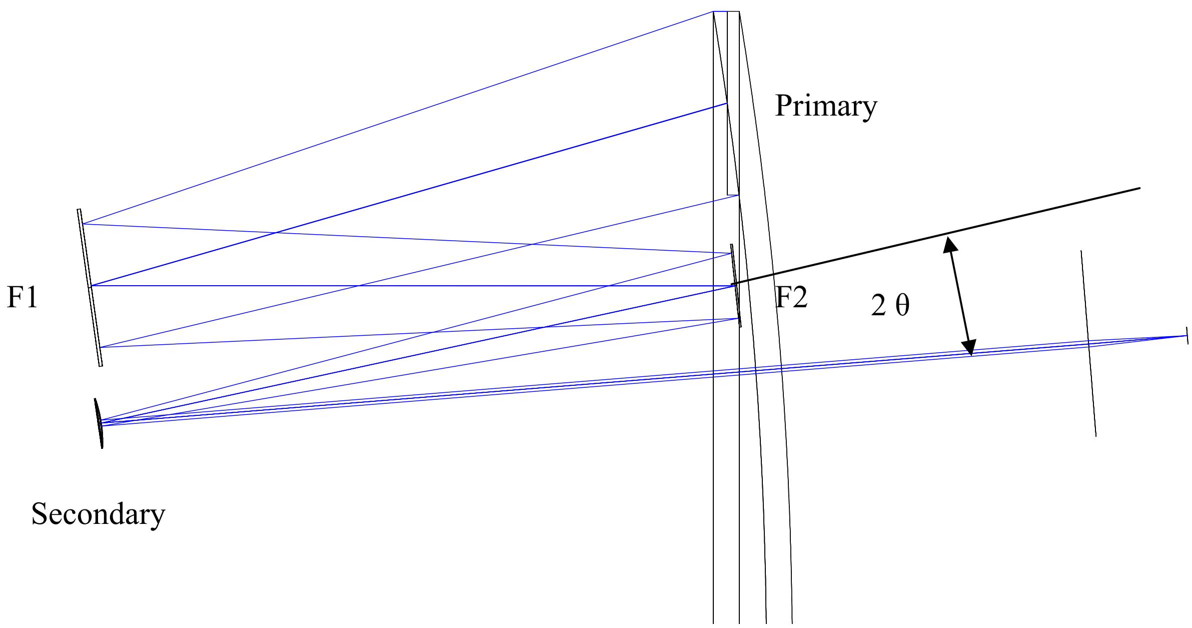

Figure 8: ZEMAX Sequential Model, 3.9 Deg Incidence Angle

3.2.1.2 Output Beam Contour

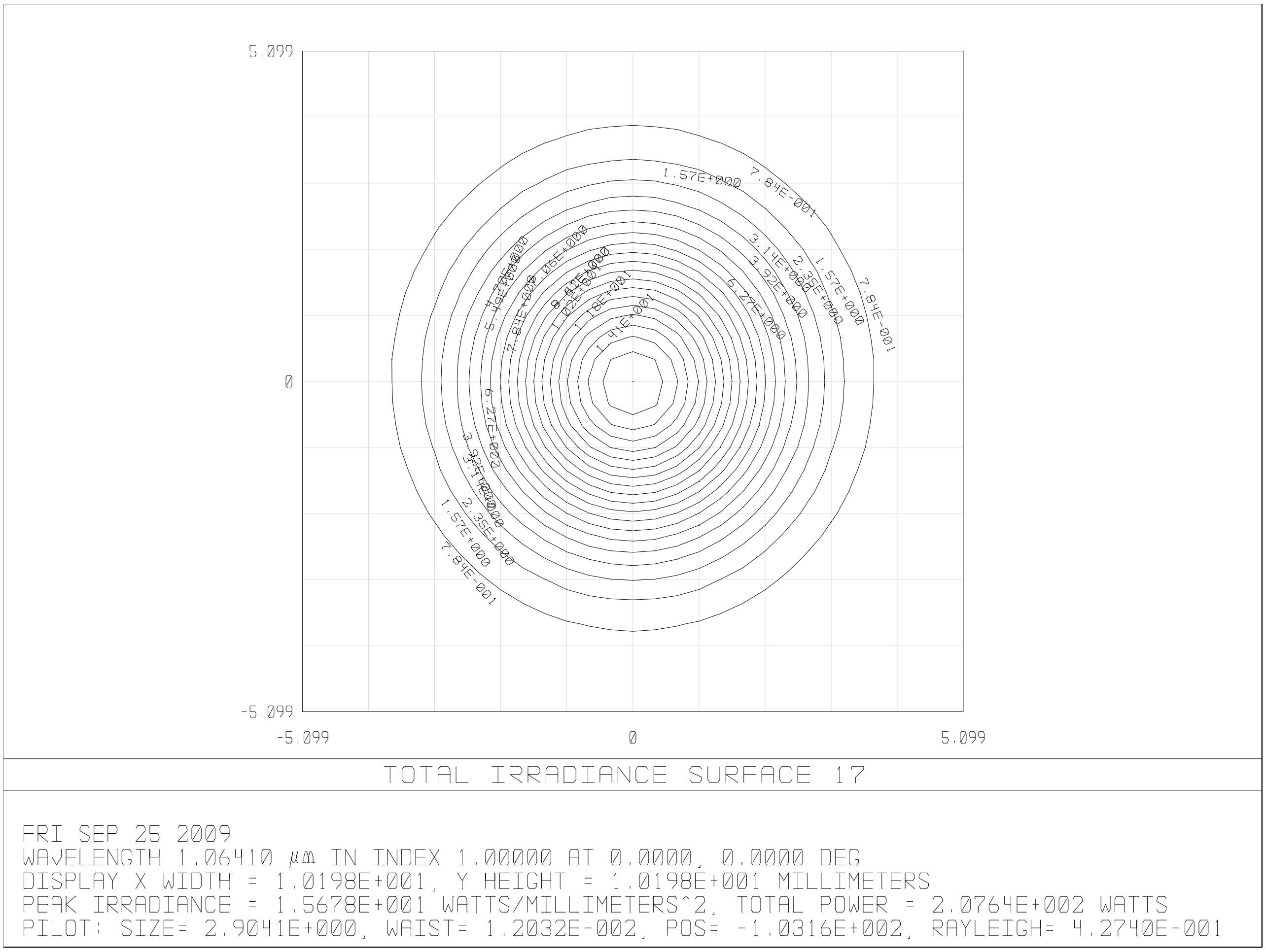

Figure 9: Physical Optics Output Beam Contour, for 3.9 Deg Incidence Angle

3.2.1.3 Wavefront Aberration

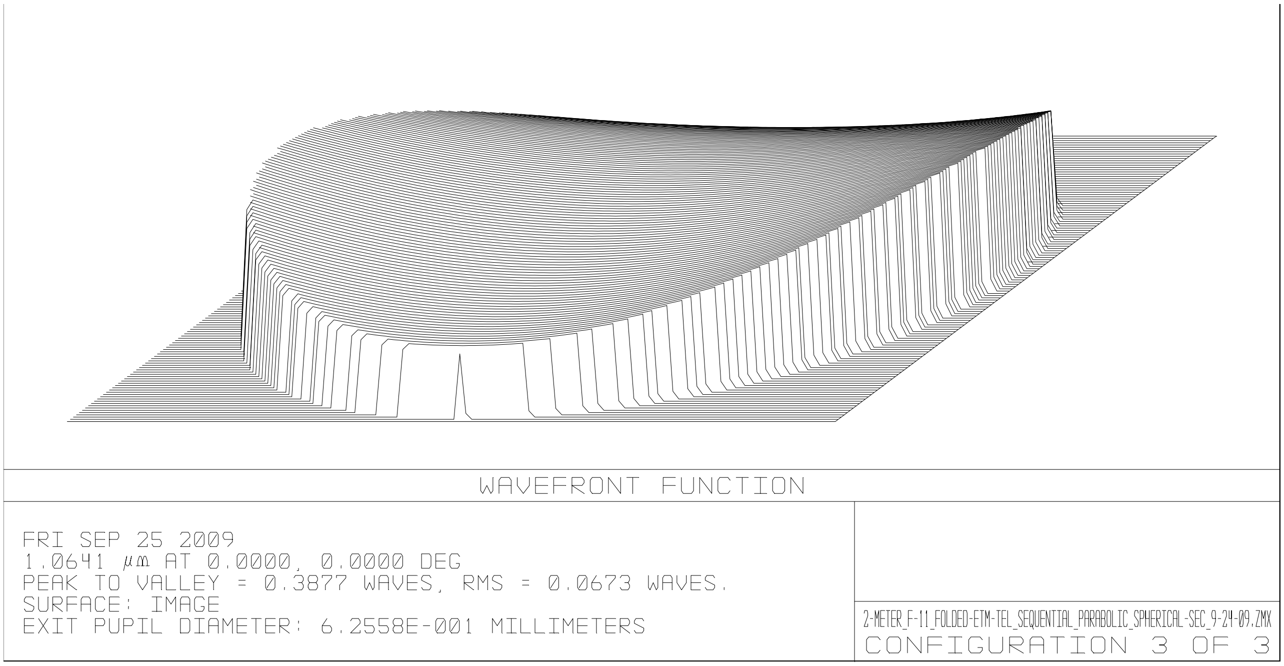

Figure 10: Wavefront Aberration, for 3.9 Deg Incidence Angle

3.2.2 Incidence Angle 5.0 Deg.

3.2.2.1 ZEMAX Sequential Model

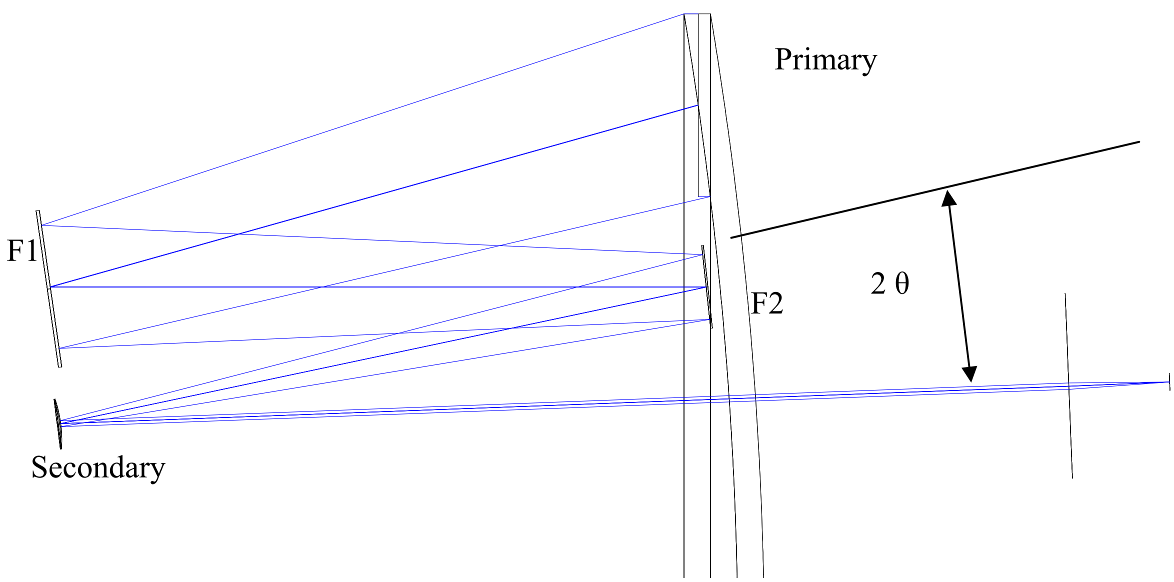

Figure 11: ZEMAX Sequential Model, 5.0 Deg Incidence Angle

3.2.2.2 Output Beam Contour

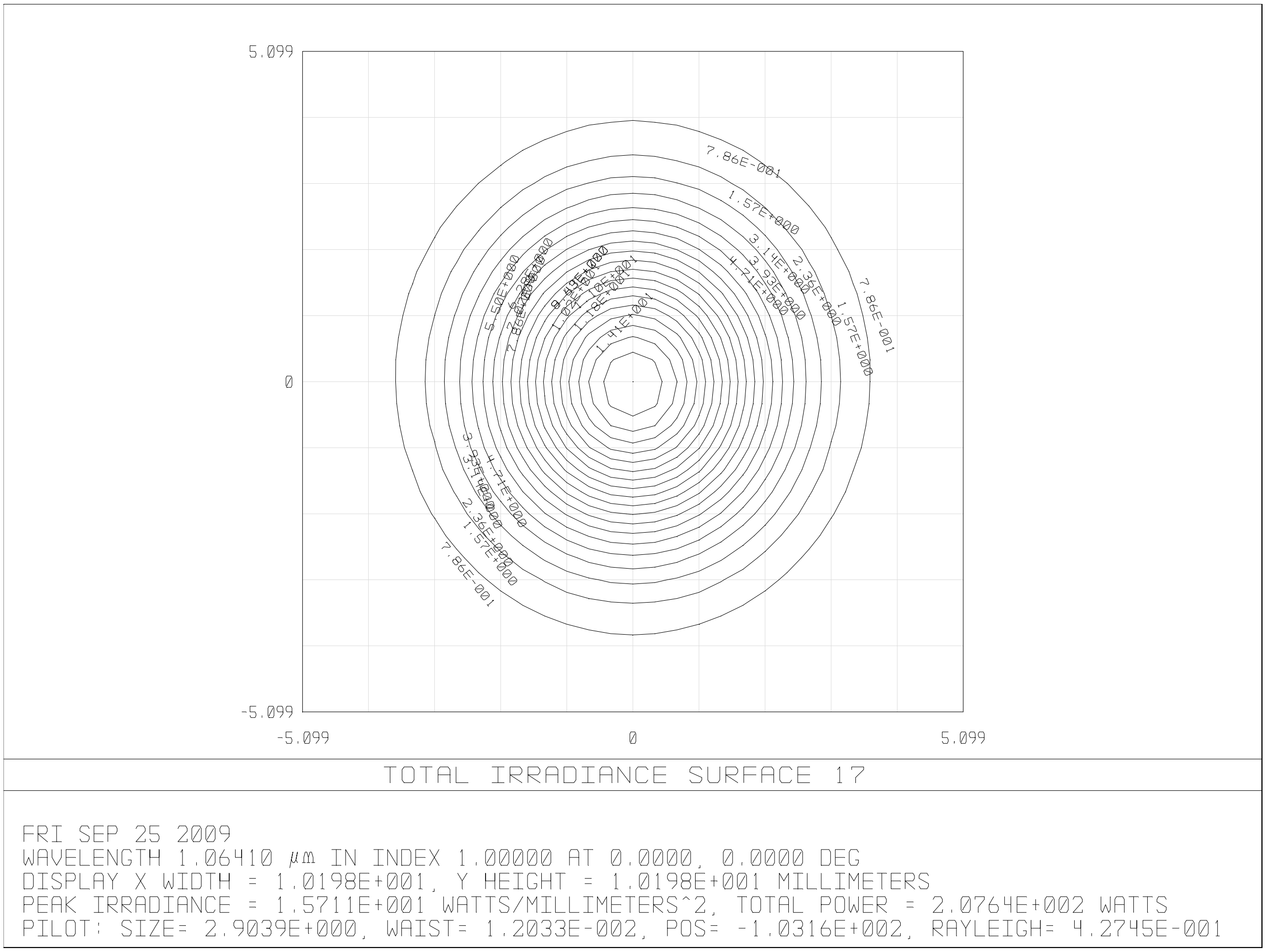

Figure 12: Physical Optics Output Beam Contour, for 5.0 Deg Incidence Angle

3.2.2.3 Wavefront Aberration

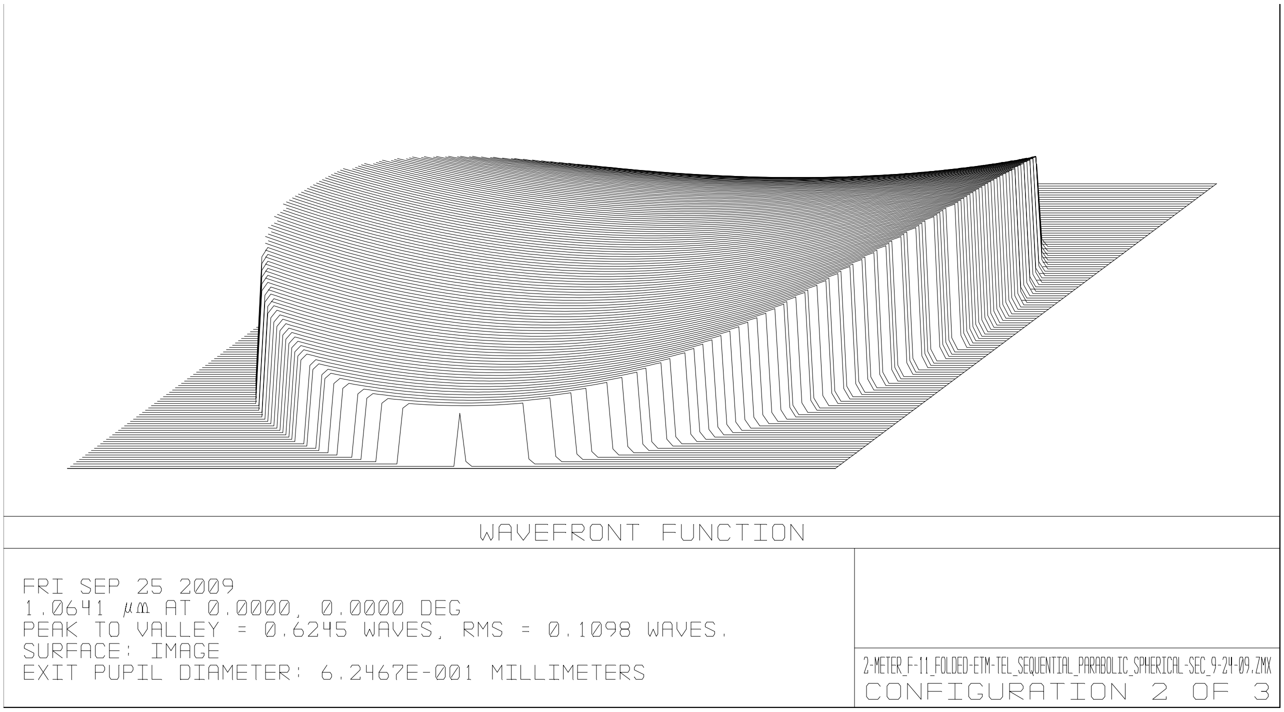

Figure 13: Wavefront Aberration, for 5.0 Deg Incidence Angle

3.2.3 Incidence Angle 6.1 Deg.

3.2.3.1 ZEMAX Sequential Model

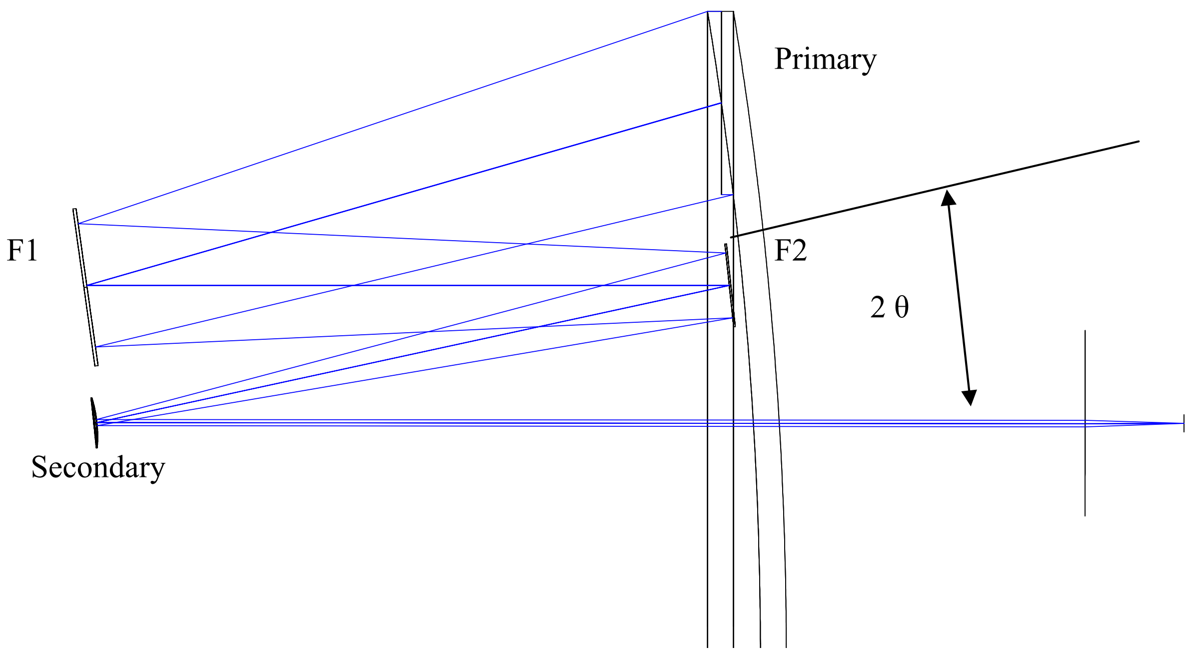

Figure 14: ZEMAX Sequential Model, 6.1 Deg Incidence Angle

3.2.3.2 Output Beam Contour

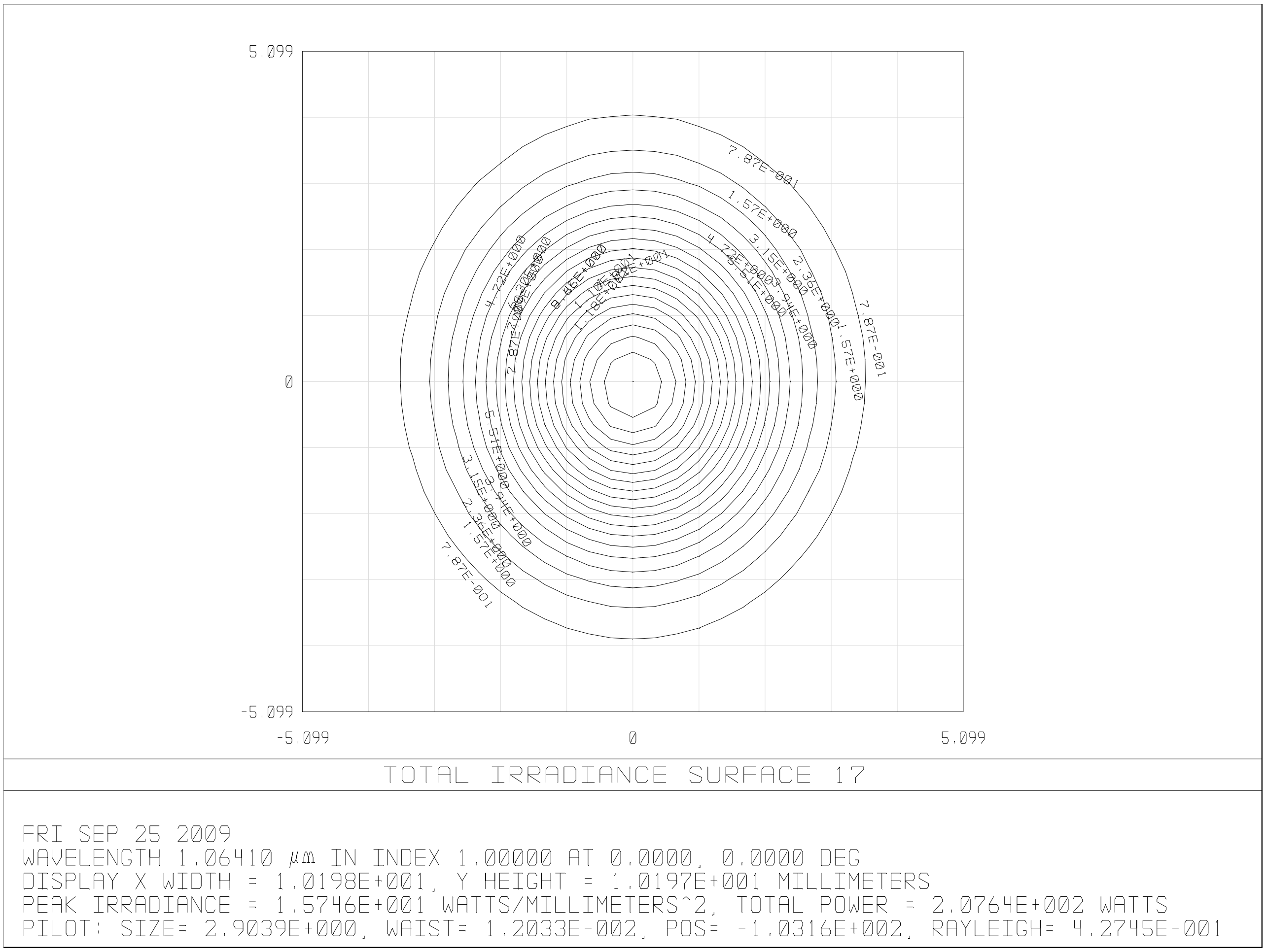

Figure 15: Physical Optics Output Beam Contour, for 6.1 Deg Incidence Angle

3.2.3.3 Wavefront Aberration

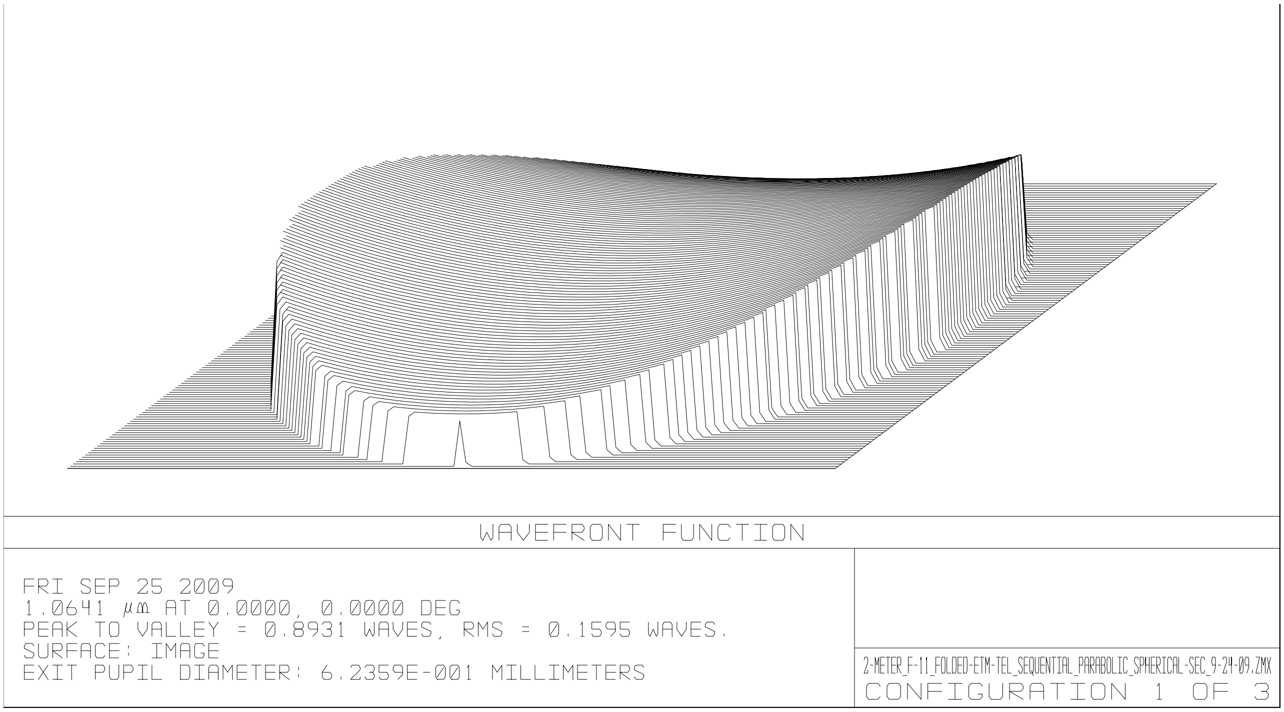

Figure 16: Wavefront Aberration, for 6.1 Deg Incidence Angle

3.2.4 Incidence Angle 4.3 Deg.

3.2.4.1 ZEMAX Sequential Model

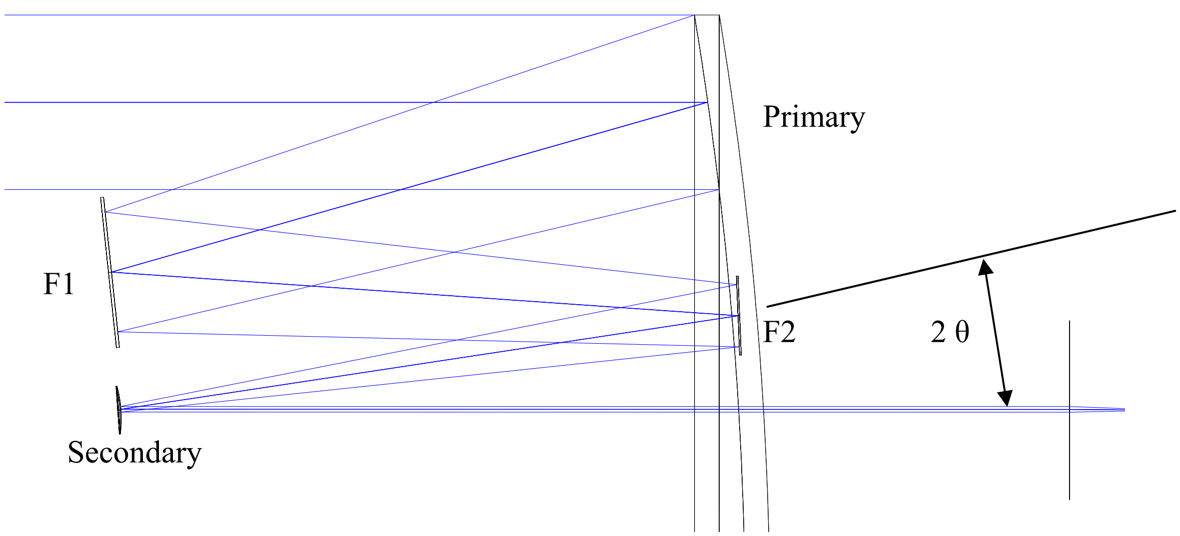

Figure 17: ZEMAX Sequential Model, 4.3 Deg Incidence Angle

3.2.4.2 Output Beam Contour

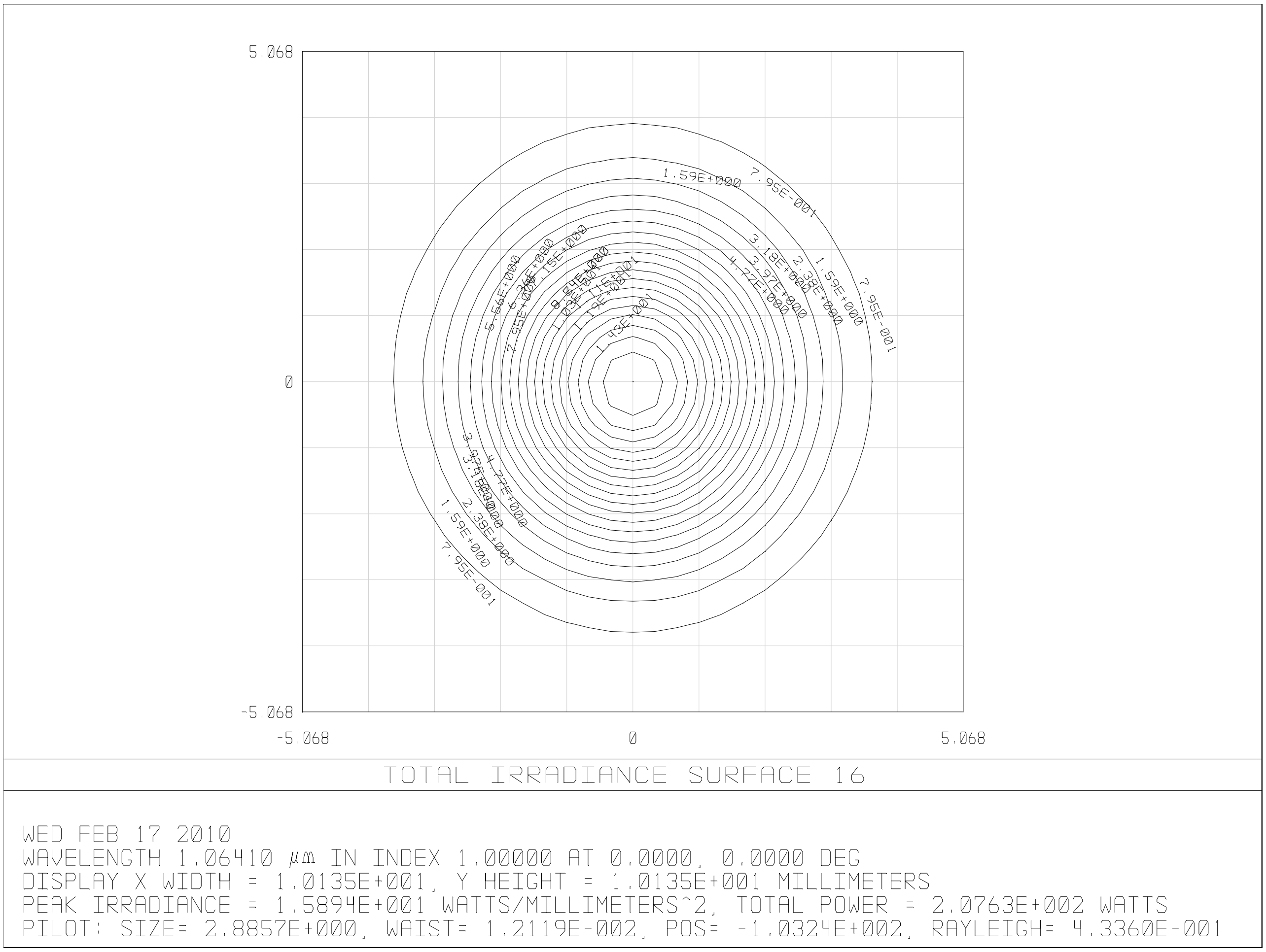

Figure 18: Physical Optics Output Beam Contour, for 4.3 Deg Incidence Angle

3.2.4.3 Spot Diagram

The telescope exhibits considerable astigmatism on axis, and with a -0.18 deg tilt of the telescope, as shown in the spot diagram.

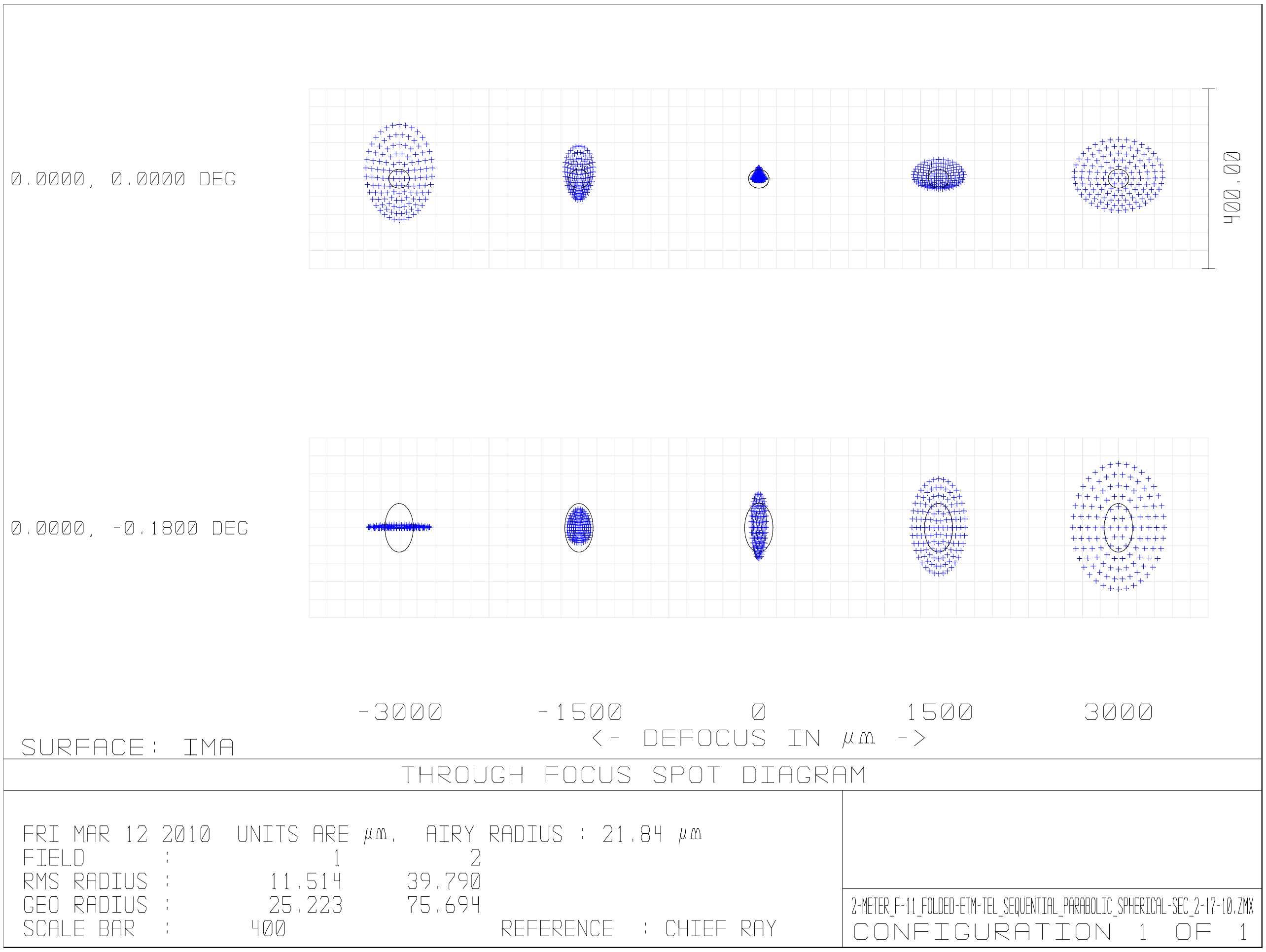

Figure 19: Spot Diagrams through Focus for 0 deg Field and -0.18 deg Field, 4.3 Deg Incidence Angle Case

3.2.4.4 Wavefront Aberration

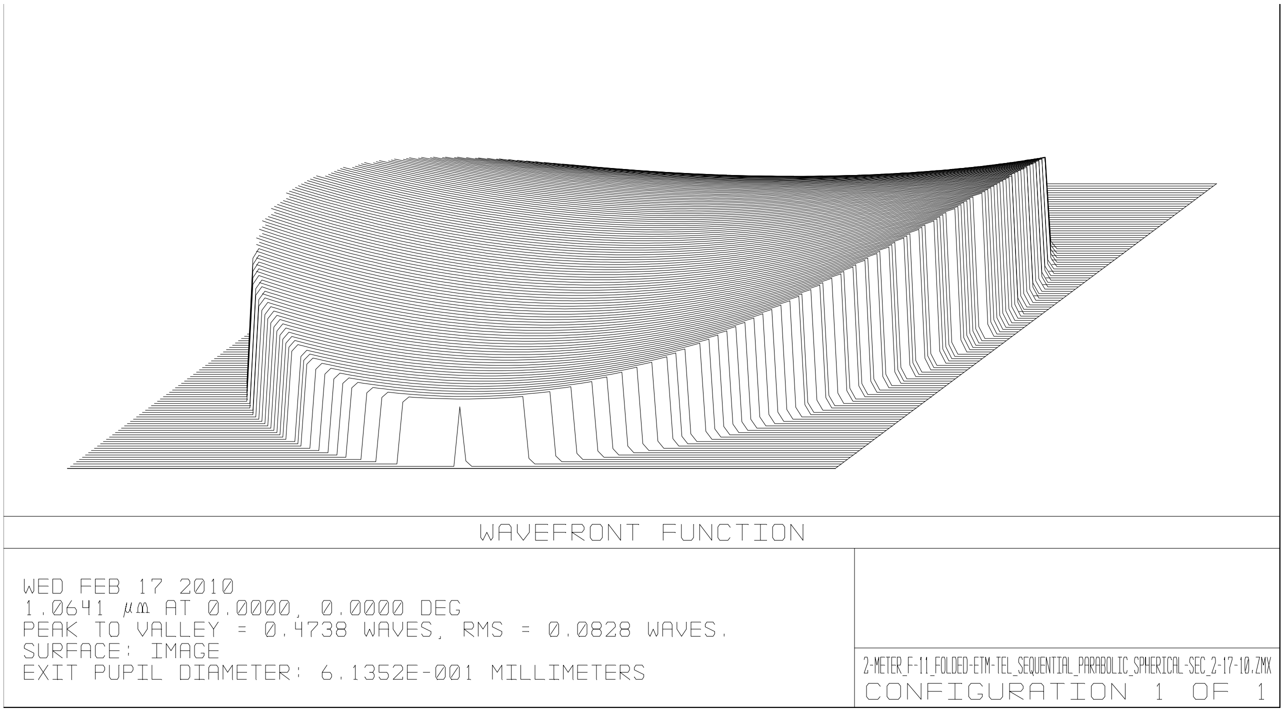

Figure 20: Wavefront Aberration, for 4.3 Deg Incidence Angle

3.2.5 Ellipticity and Aberration vs Incidence Angle on Secondary Spherical Mirror

The ellipticity was measured from the beam contour plots and is summarized in Table 2: Ellipticity and Aberration vs Incidence Angle.

Table 2: Ellipticity and Aberration vs Incidence Angle, Spherical Secondary

Incidence Angle, Deg	**Ellipticity**	**Aberration, waves peak to valley**
3.9	1.048	0.3877
4.3 (note)	1.063	0.474
5.0	1.081	0.6245
6.1	1.12	0.8931

Note: The 4.3 degree case is for the proposed telescope beam configuration, which is slightly different from the other cases, with a secondary mirror focal length of 65.4 mm, instead of 66.7 mm.

3.2.6 4.3 Deg Incidence Angle Case: Effect of Telescope Tilt

Table 3: 4.3 Deg Incidence Angle Case: Ellipticity and Aberration vs Telescope Tilt

Telescope Tilt, Deg	**Ellipticity**	**Aberration, waves peak to valley**
0	1.07	0.4771
-0.05	1.03	0.1968
-0.1	1.19	0.3586
-0.18	1.57	0.3932
0.05	1.10	0.7716
0.1	1.05	0.9126
0.18	1.09	0.5986

3.3 Hybrid: Parabolic Mirror Primary with 150mm EFL Triplet Lens Secondary

3.3.1 ZEMAX Sequential Model

The ZEMAX model is shown in Figure 4.

3.3.2 Output Beam Contour

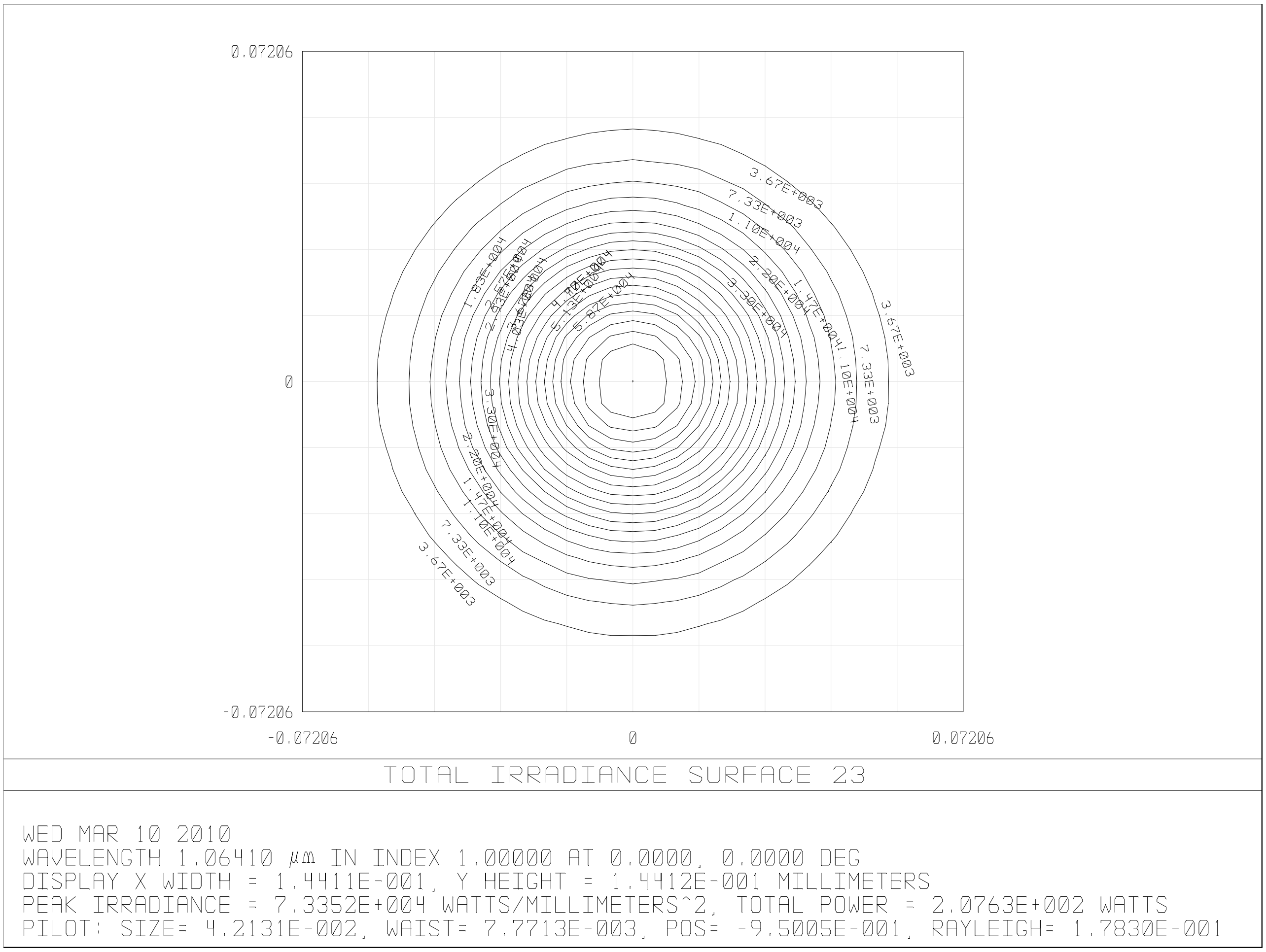

Figure 21: Physical Optics Output Beam Contour, Parabolic Primary with 150mm EFL Triplet Lens Secondary

3.3.3 Spot Diagram

The telescope is well behaved on axis, but exhibits considerable astigmatism with a -0.18 deg tilt.

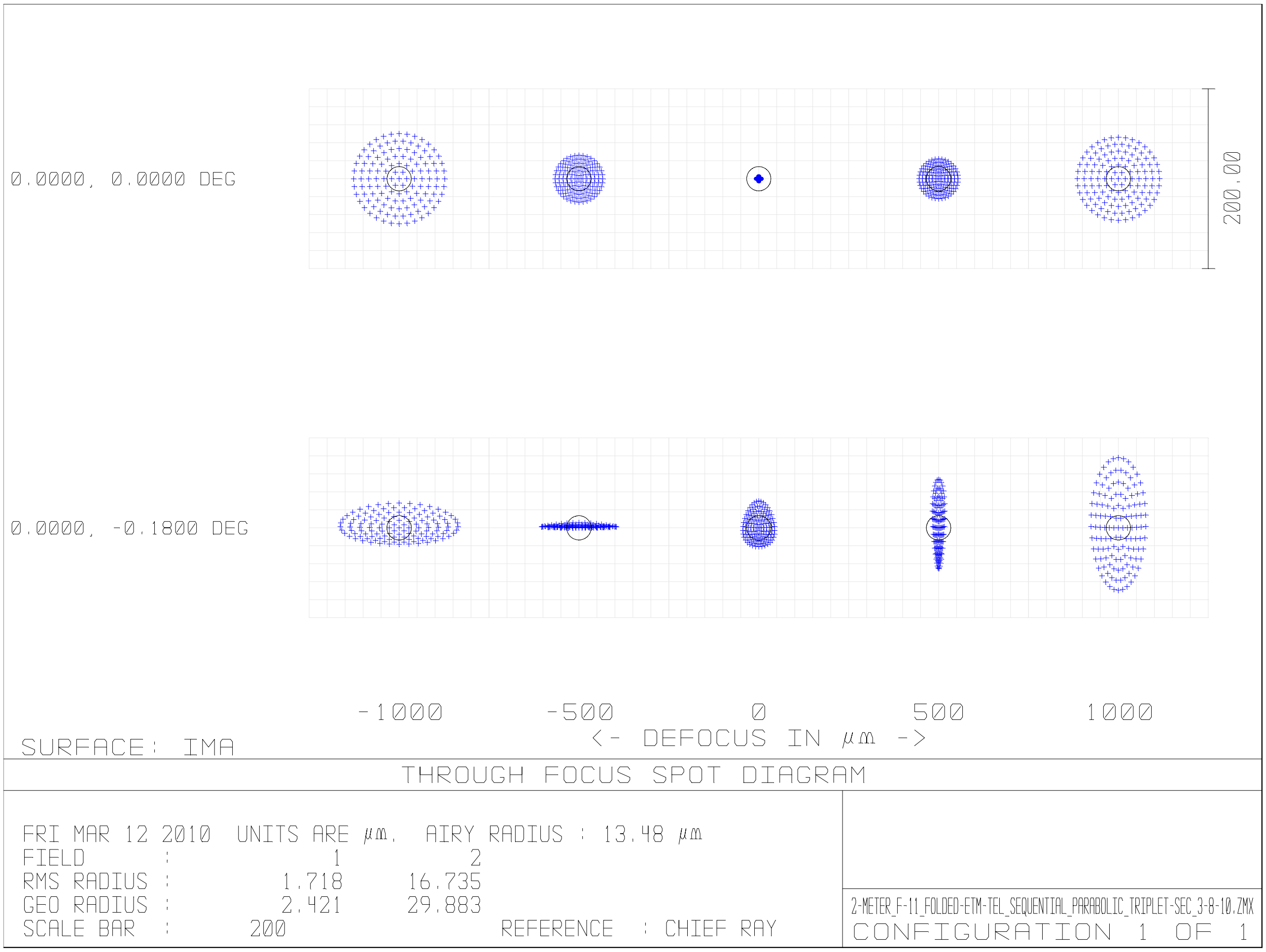

Figure 22: Spot Diagrams through Focus for 0 deg Field and -0.18 deg Field, 150mm EFL Triplet Lens Secondary Case

3.3.4 Wavefront Aberration

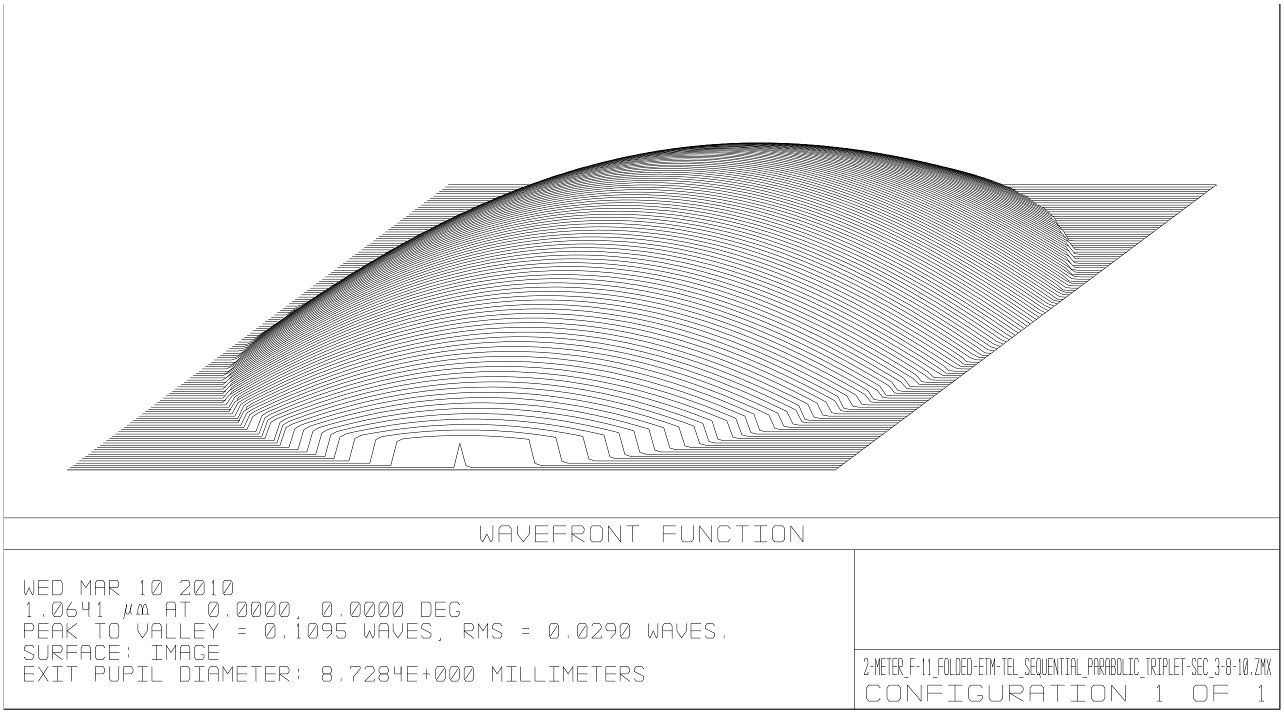

Figure 23: Wavefront Aberration, Parabolic Primary with 150mm EFL Triplet Lens Secondary

3.3.5 150mm EFL Triplet Lens Secondary Case: Effect of Telescope Tilt

Table 4: Ellipticity and Aberration vs Telescope Tilt, 150mm EFL Triplet Lens Secondary Case

Telescope Tilt, Deg	Ellipticity	Aberration, waves peak to valley
0	1.000	0.1095
-0.05	1.34	0.5355
-0.1	1.71	1.1001
-0.18	3.35	2.1071
0.1	1.51	0.8663
0.05	1.22	0.4472

3.4 Hybrid: Parabolic Mirror Primary with 125mm EFL Triplet Lens Secondary

3.4.1 ZEMAX Sequential Model

The ZEMAX model is shown in Figure 4.

3.4.2 Output Beam Contour

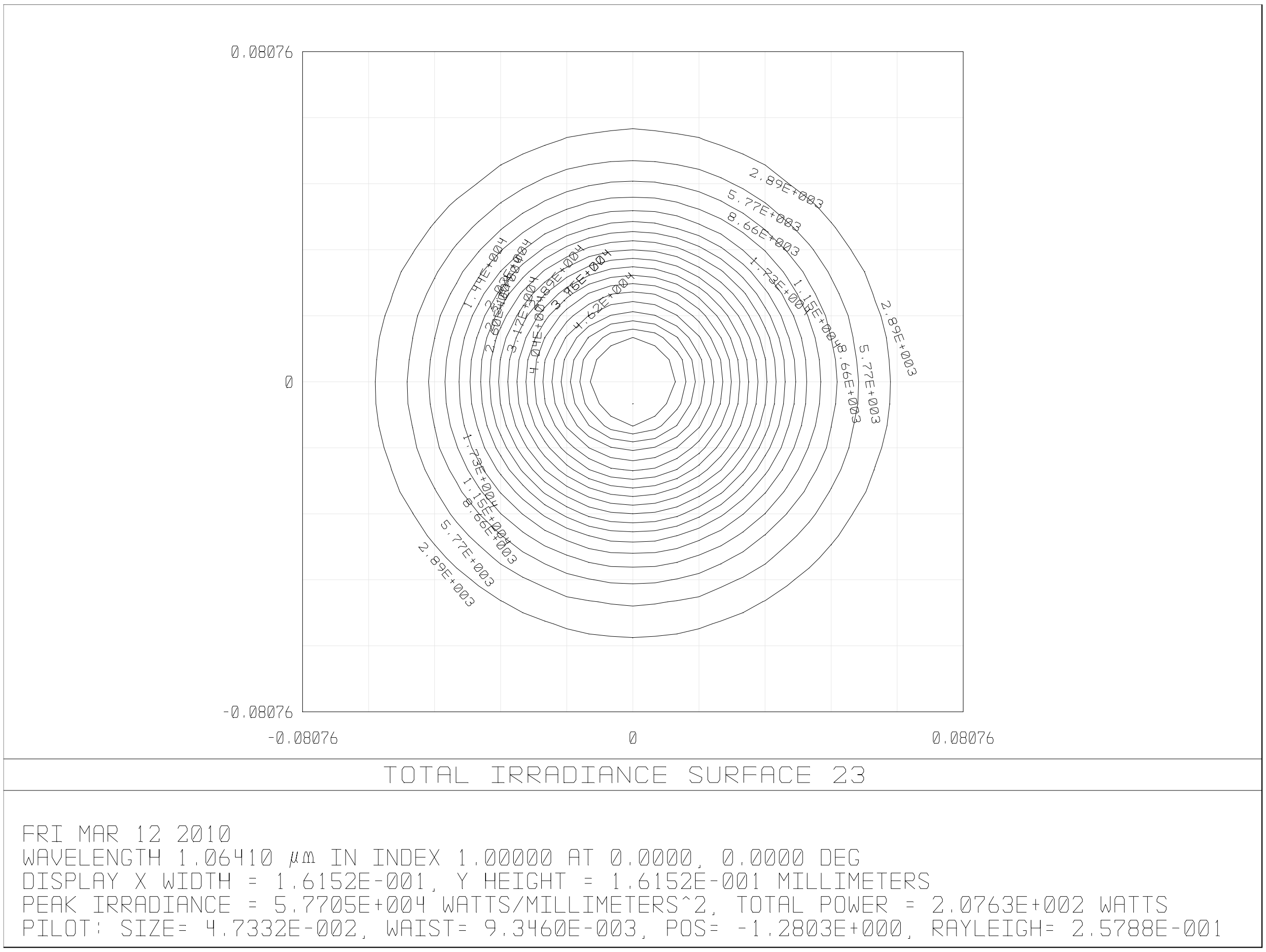

Figure 24: Physical Optics Output Beam Contour, Parabolic Primary with 125mm EFL Triplet Lens Secondary

3.4.3 Spot Diagram

The telescope is well behaved on axis, but exhibits considerable astigmatism with a -0.18 deg tilt.

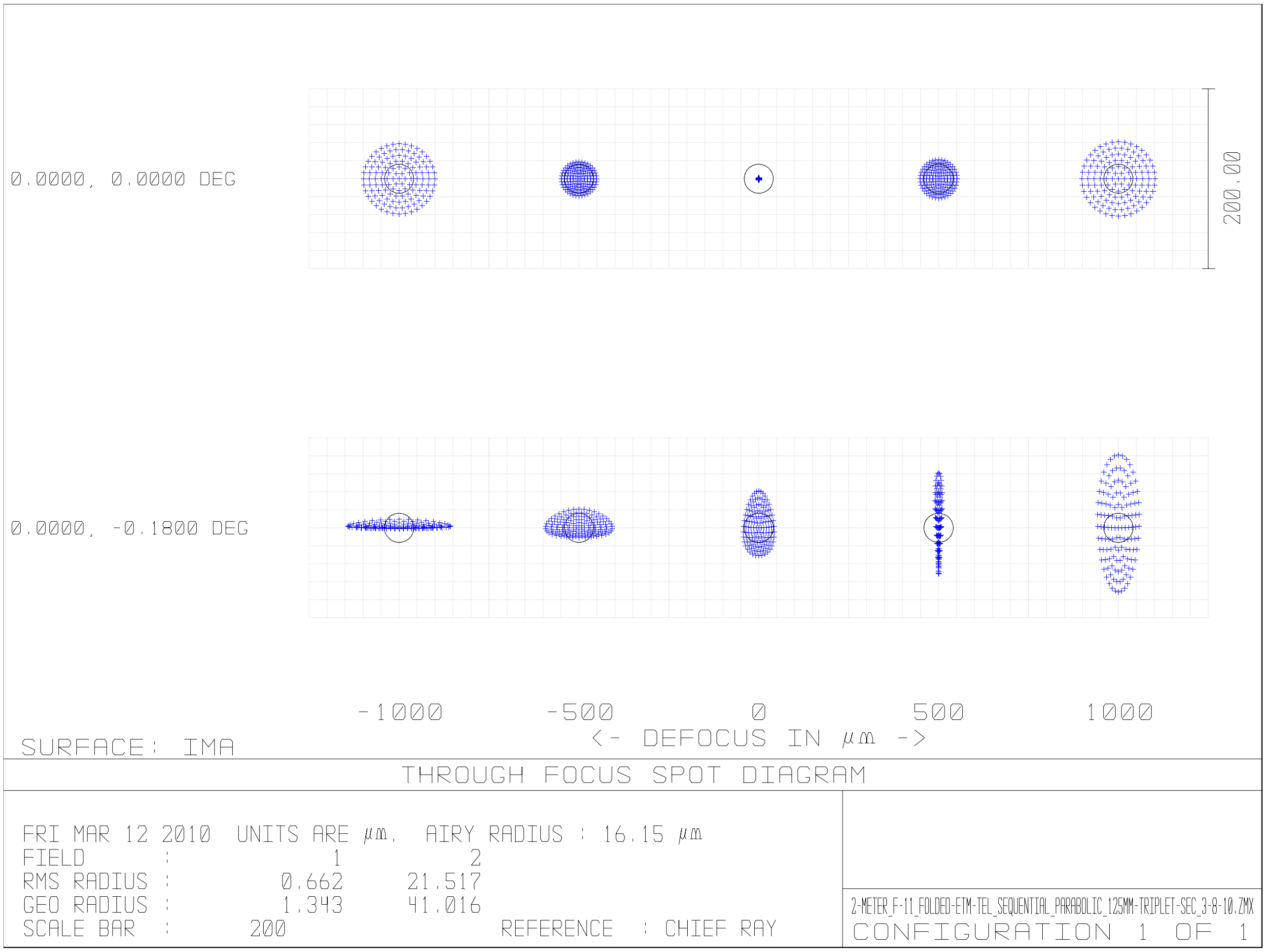

Figure 25: Spot Diagrams through Focus for 0 deg Field and -0.18 deg Field, 125mm EFL Triplet Lens Secondary Case

3.4.4 Wavefront Aberration

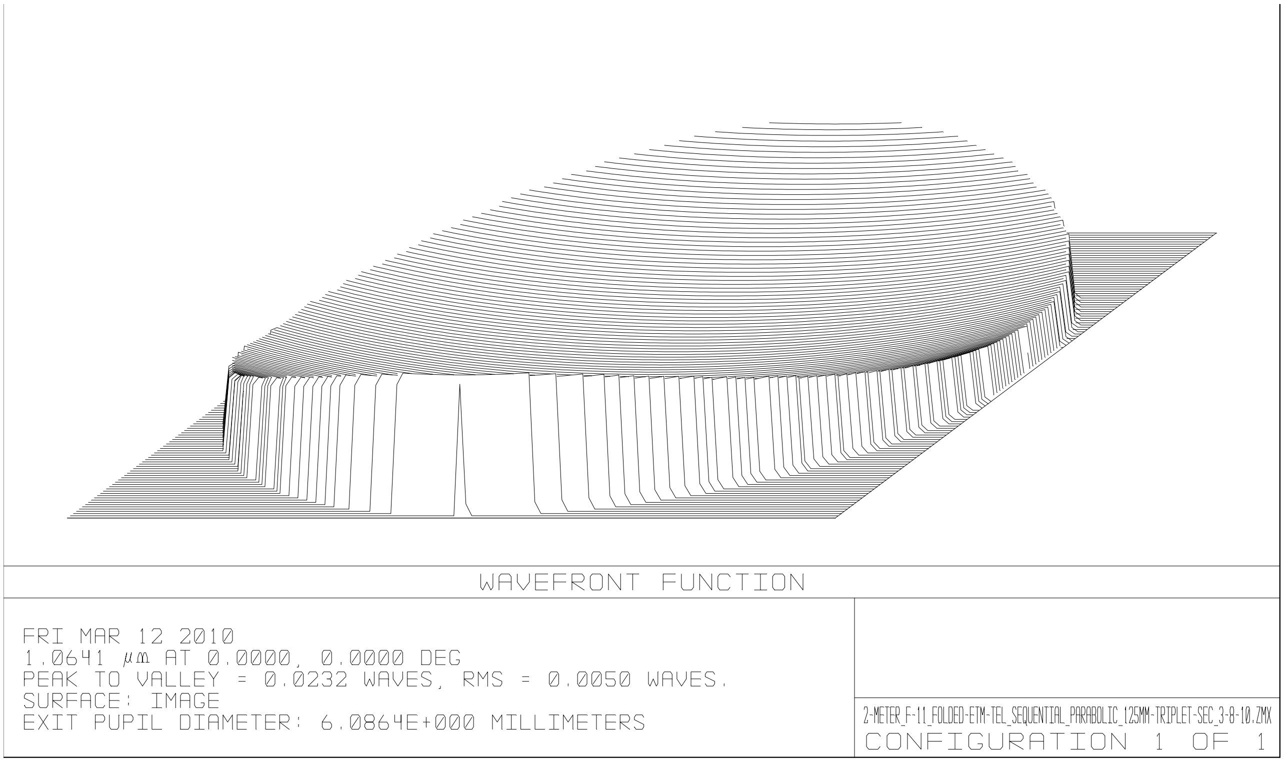

Figure 26: Wavefront Aberration, Parabolic Primary with 125mm EFL Triplet Lens Secondary

4 Comparison of Off-axis Parabolas with the Hybrid Telescope for the Hartmann Reference Beam

The Hartman Reference beam reflects from the outer surface of the reaction mass of the ETM mirror suspension. This beam is incident on the primary mirror of the telescope with a maximum angle of approximately -0.18 degrees in the plane of the telescope mirrors.

The green beam in the figures is the 0.532 nm Hartmann reference beam.

The contour of the Hartman reference beam at the output of the telescope was calculated using the Physical Optics Propagation program as before, by launching a Gaussian beam with a waist of 8.3mm located a distance 2E6 mm in front of the ETM telescope. The telescope was tilted by -0.18 deg about an axis located at the AR surface of the ETM mirror to simulate the input angle of the Hartmann reference beam that reflects from the 0.1 deg vertically tilted AR surface of the ETM.

4.1 Off-axis Parabolic Telescope

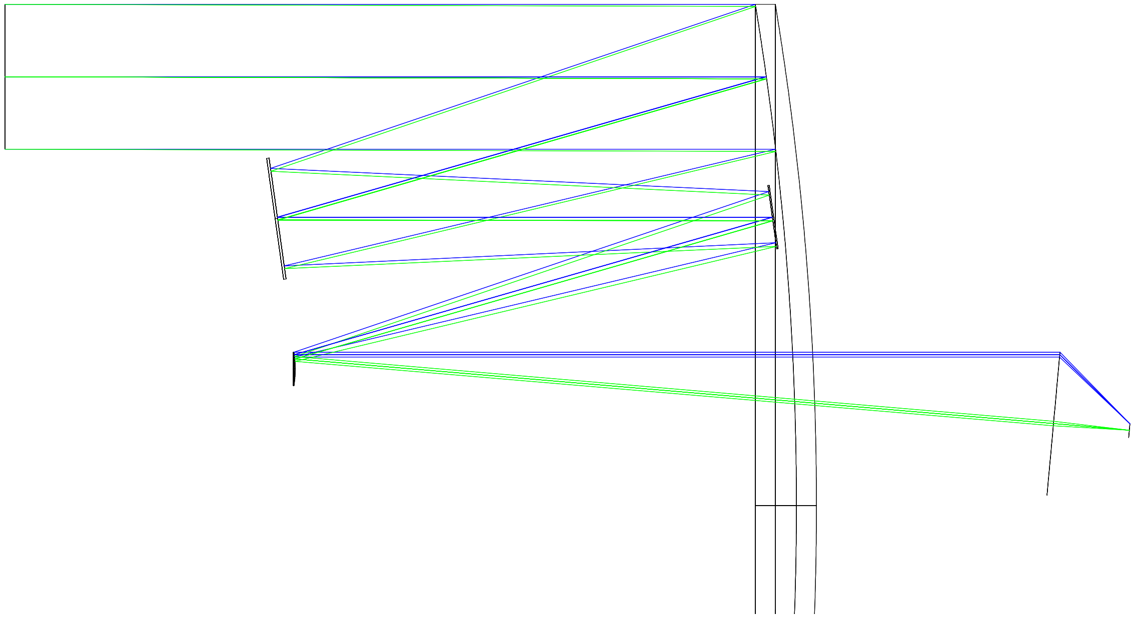

Figure 27: ZEMAX Sequential Model, Off-axis Parabolic

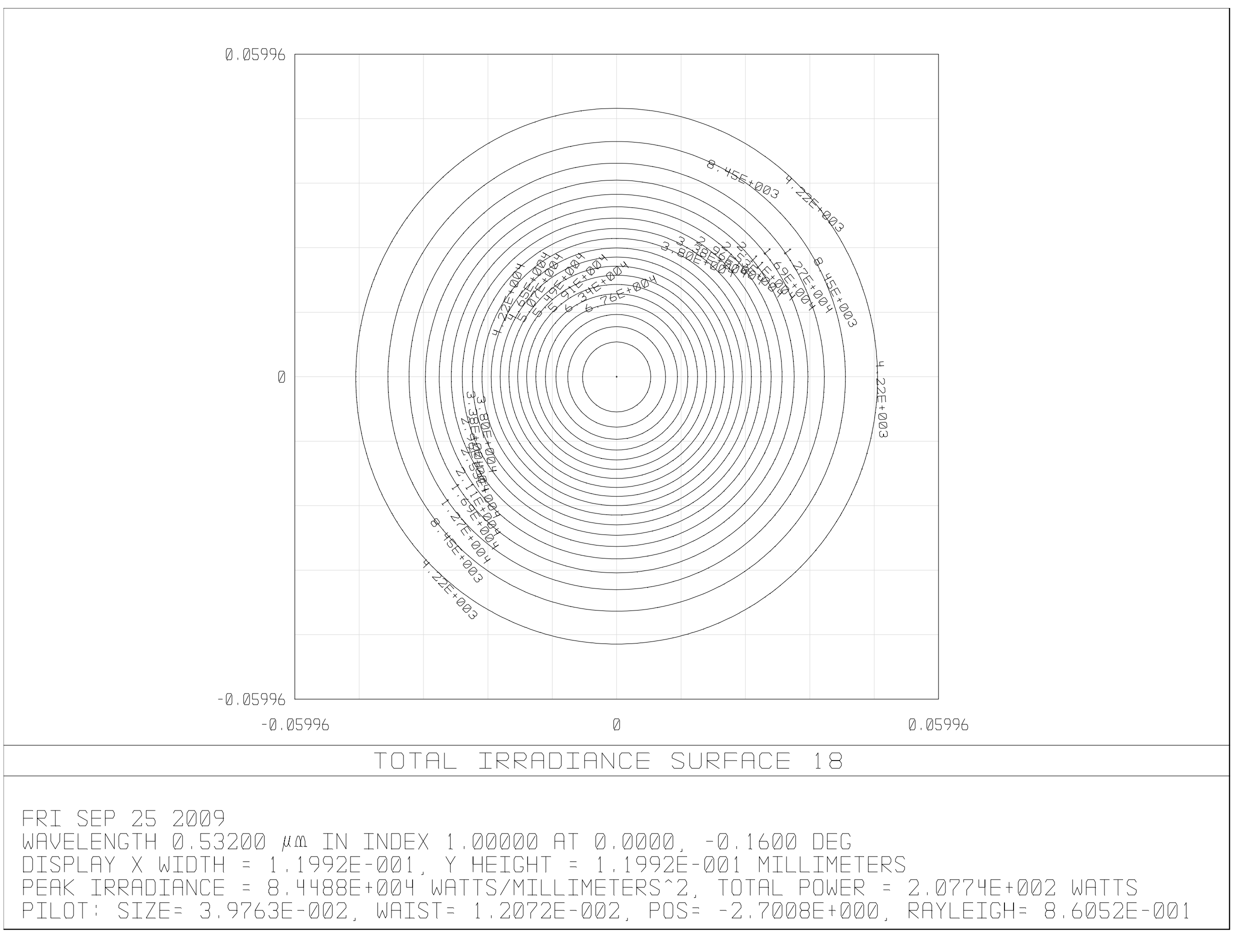

Figure 28: Physical Optics Hartmann Beam Contour, for Off-axis Parabolic

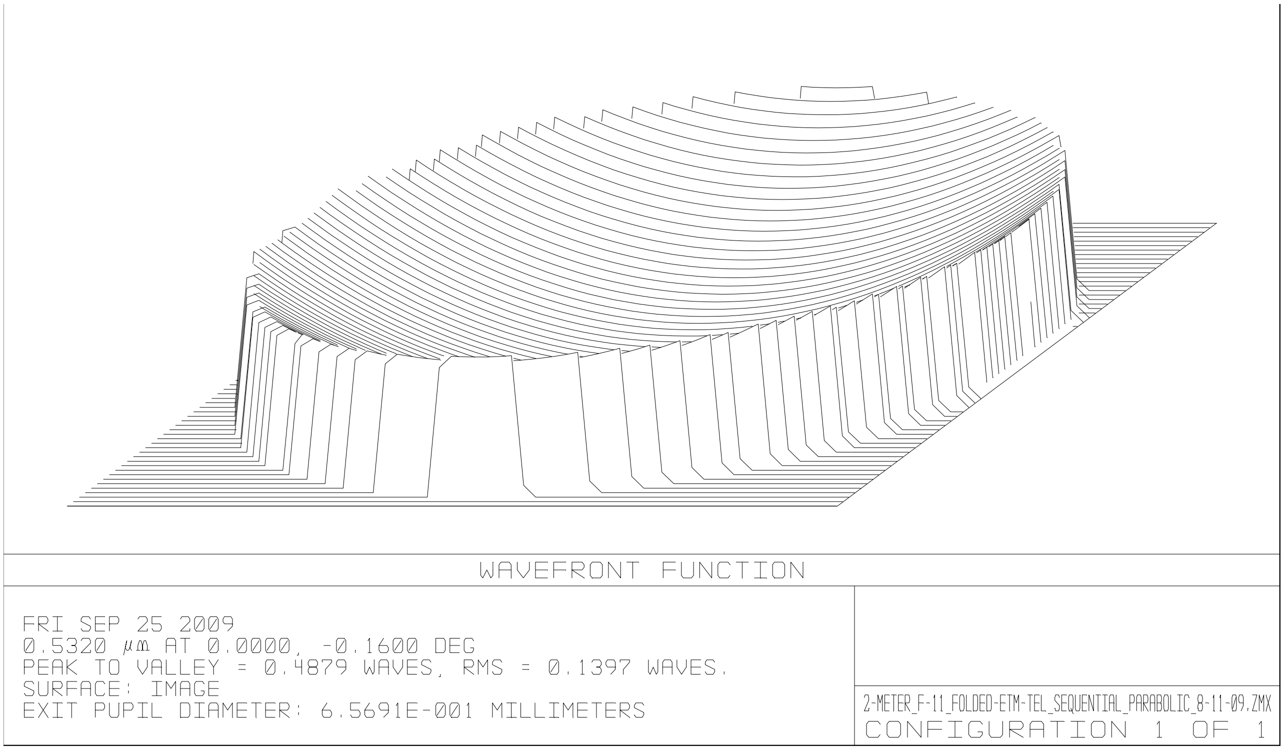

Figure 29: Wavefront Aberration of Hartmann Beam, for Off-axis Parabolic

4.2 Hybrid Telescope, Spherical Secondary with 4.3 Degree Incidence Angle

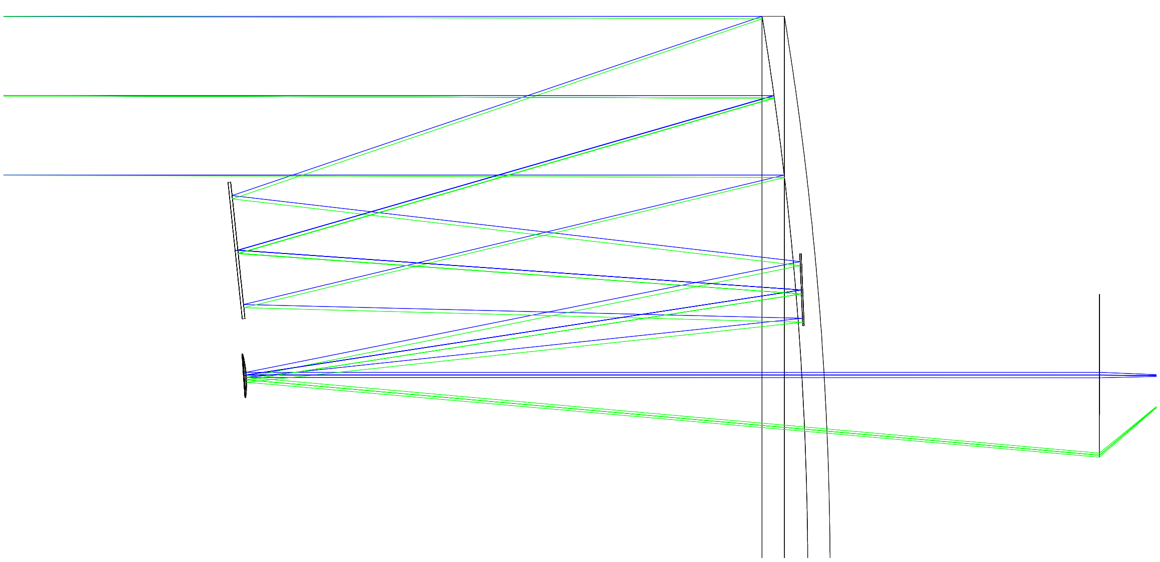

Figure 30: ZEMAX Sequential Model, 4.3 Deg Incidence Angle Spherical Secondary

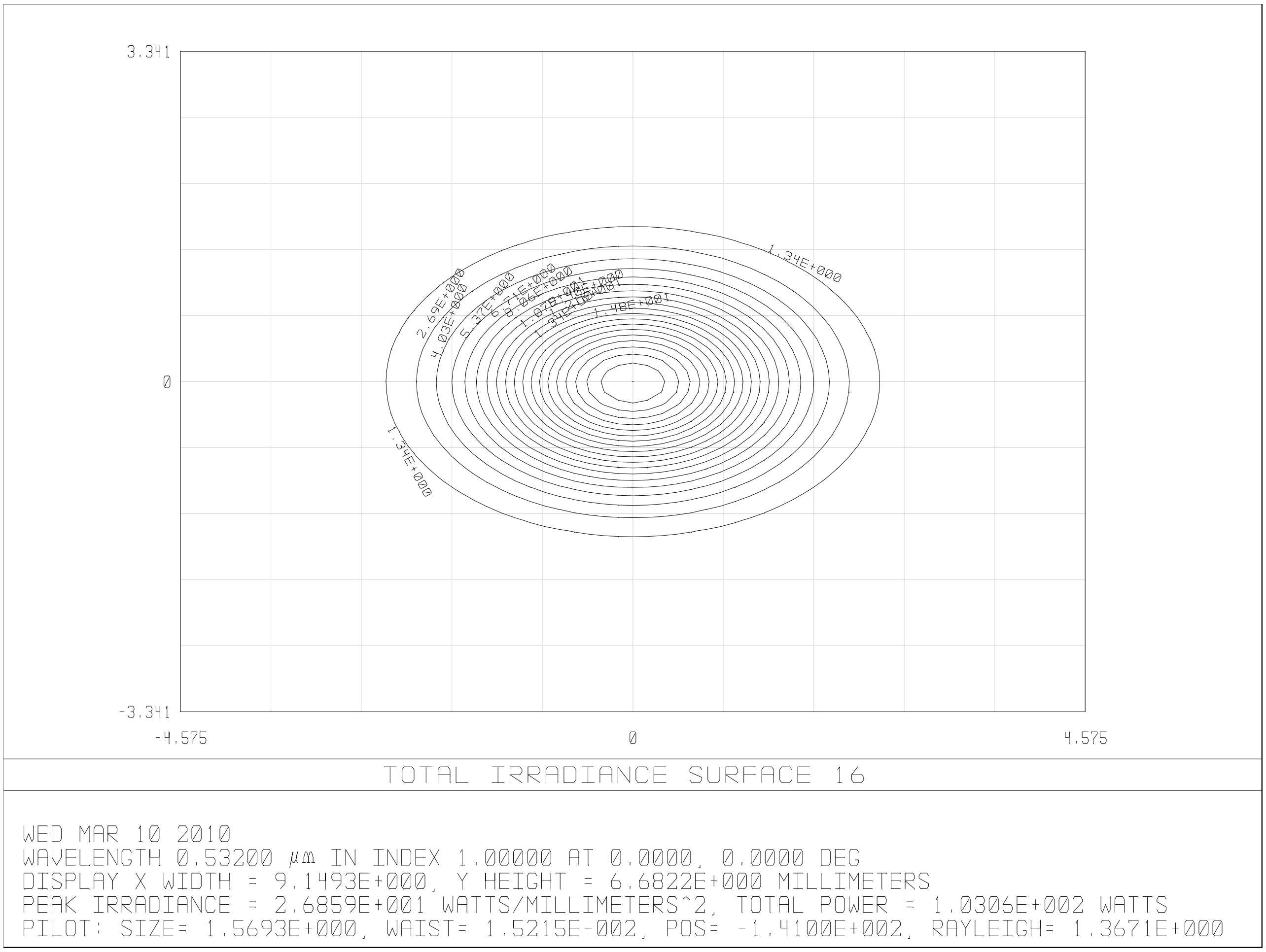

Figure 31: Physical Optics Hartmann Beam Contour, for 4.3 Deg Incidence Angle Spherical Secondary

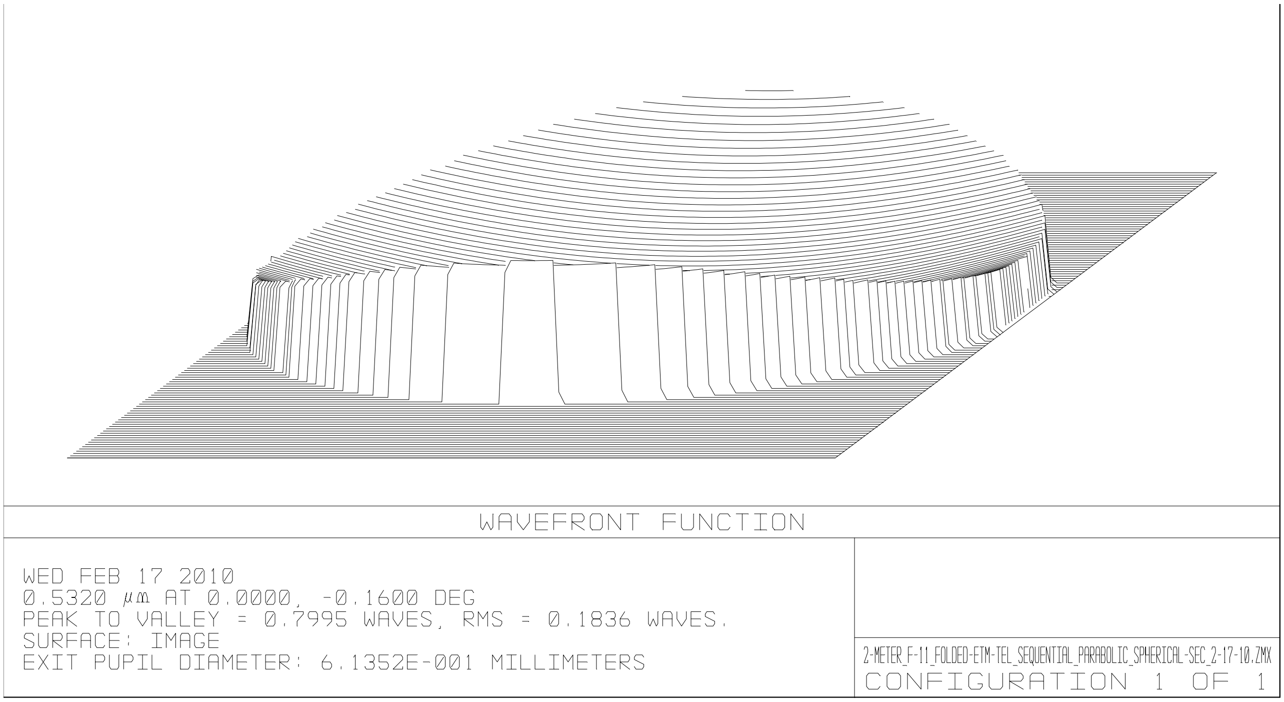

Figure 32: Wavefront Aberration Hartmann Beam, for 4.3 Deg Incidence Angle Spherical Secondary

4.3 Hybrid: Parabolic Mirror Primary with 150mm EFL Triplet Lens Secondary Design

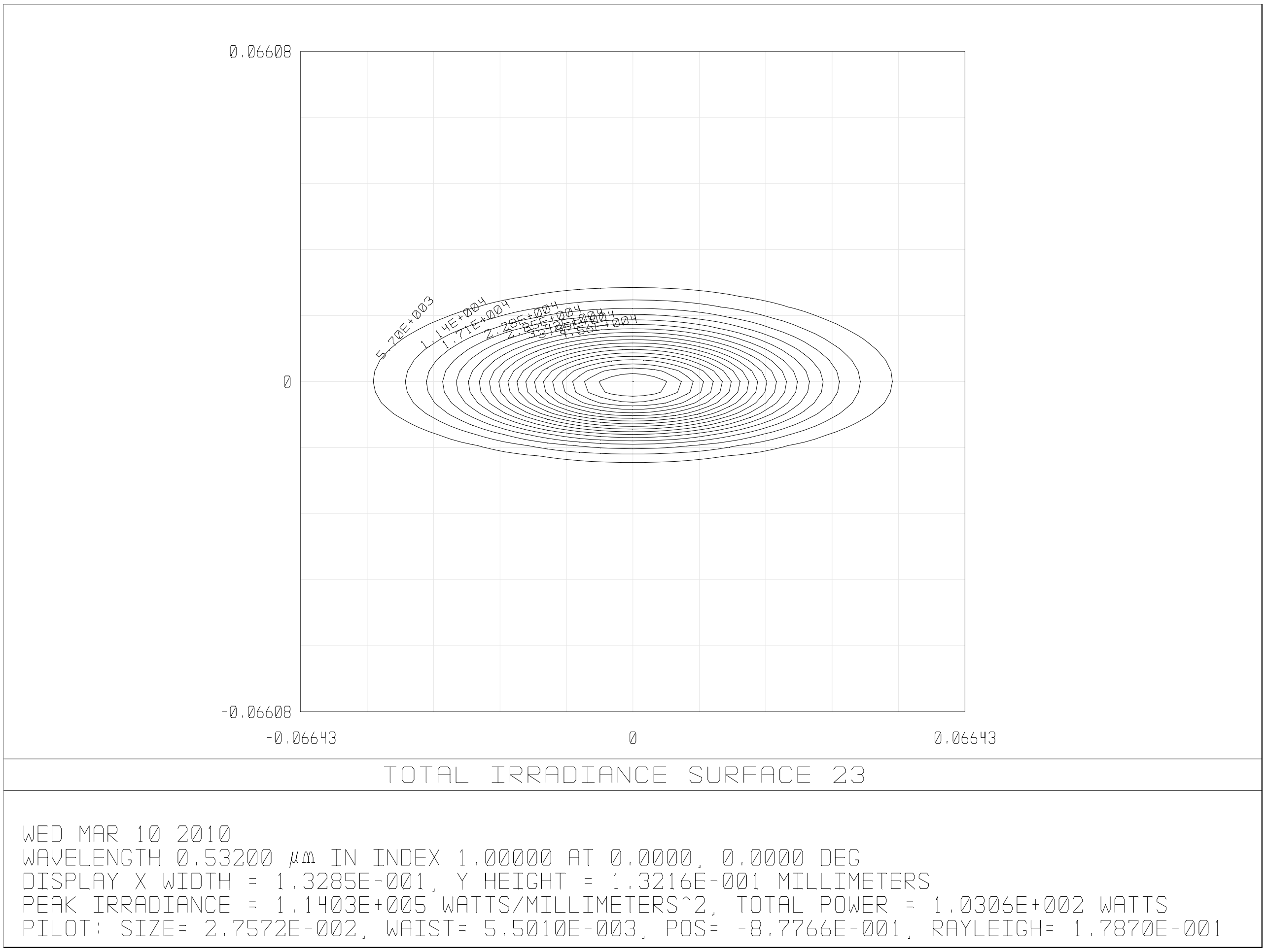

Figure 33: Physical Optics Hartmann Beam Contour, for Parabolic Mirror Primary with 150mm EFL Triplet Lens Secondary

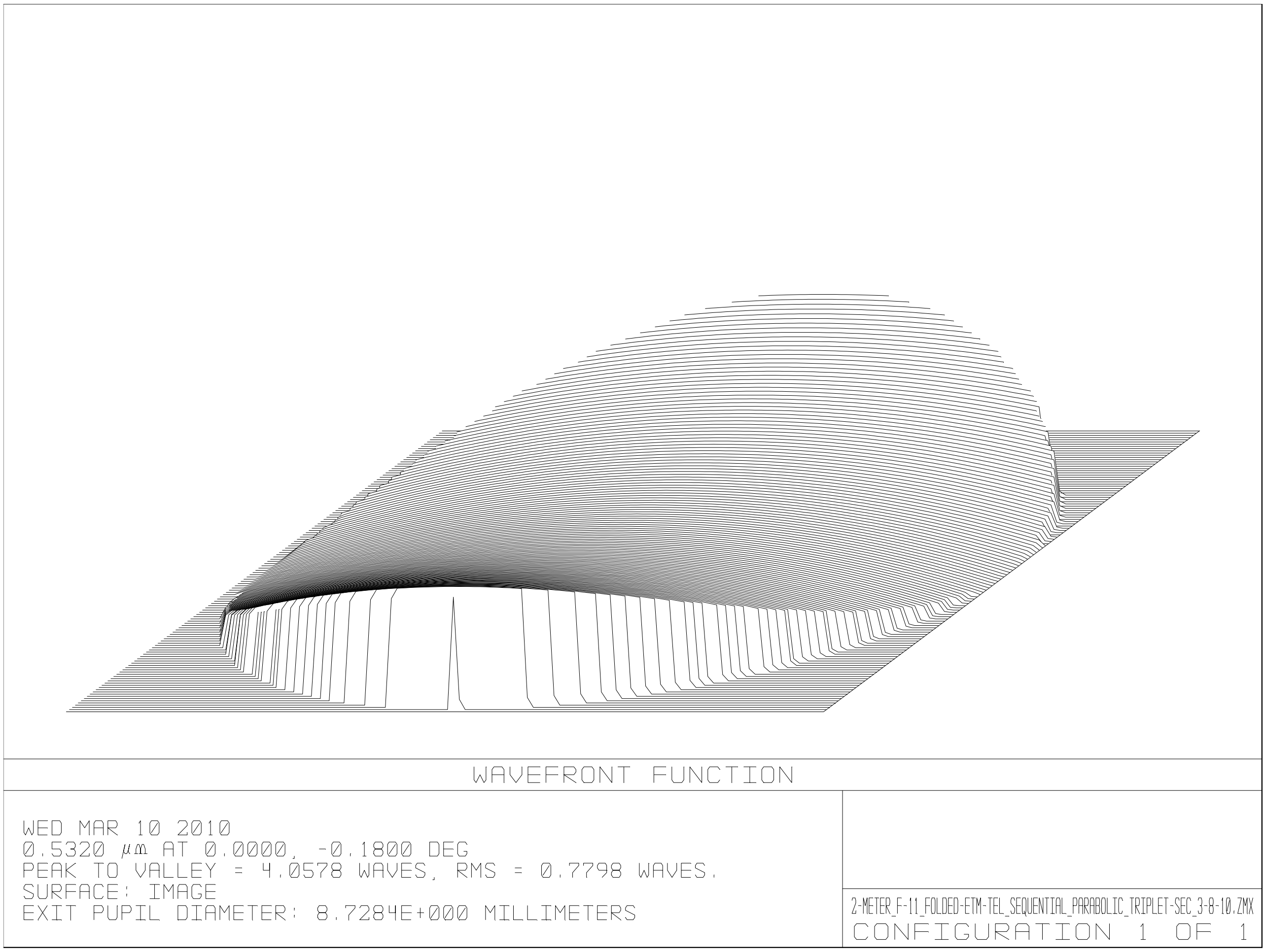

Figure 34: Wavefront Aberration Hartmann Beam, for Parabolic Mirror Primary with 150mm EFL Triplet Lens Secondary

4.4 Hybrid: Parabolic Mirror Primary with 125mm EFL Triplet Lens Secondary Design

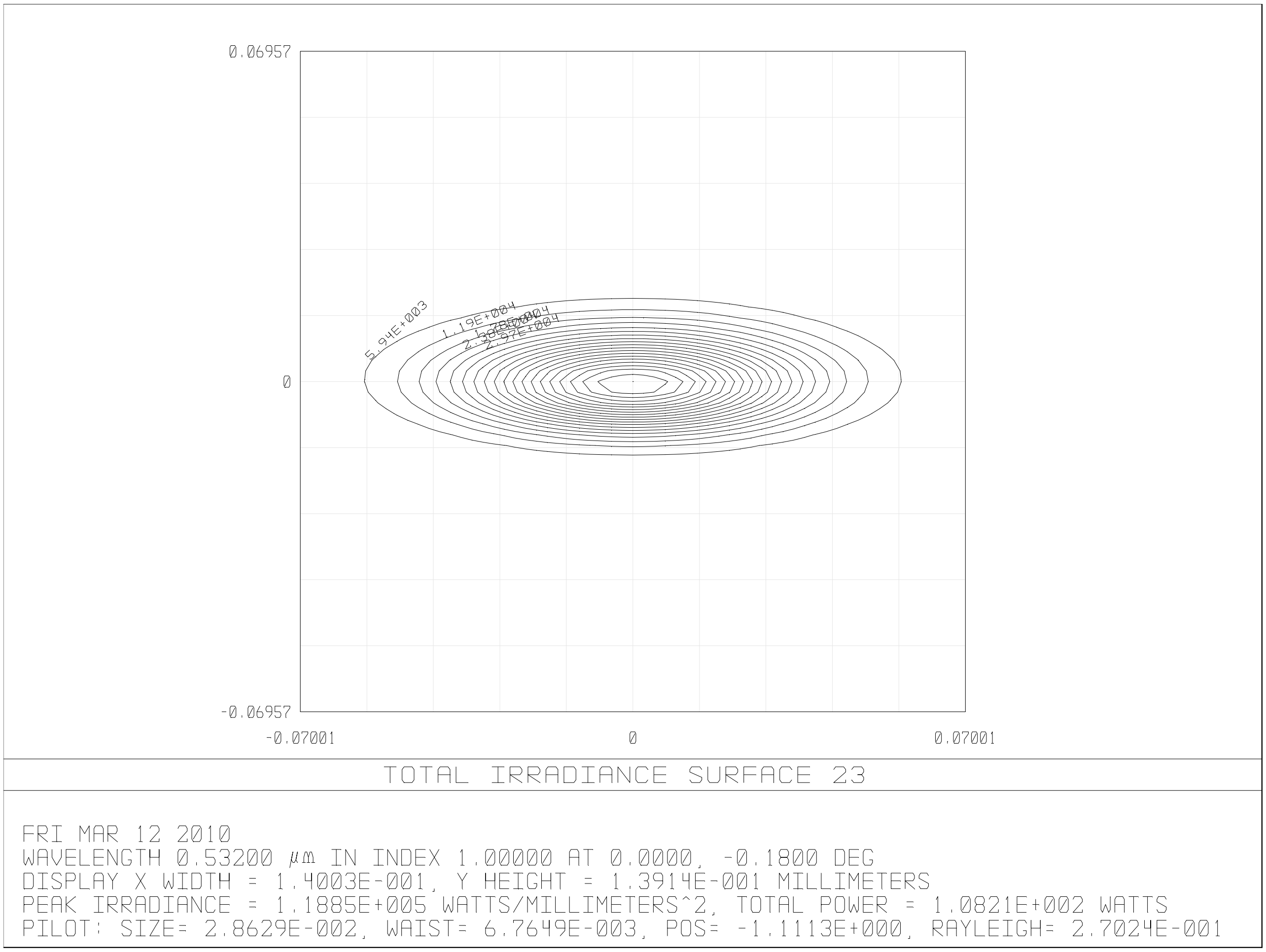

Figure 35: Physical Optics Hartmann Beam Contour, for Parabolic Mirror Primary with 125mm EFL Triplet Lens Secondary

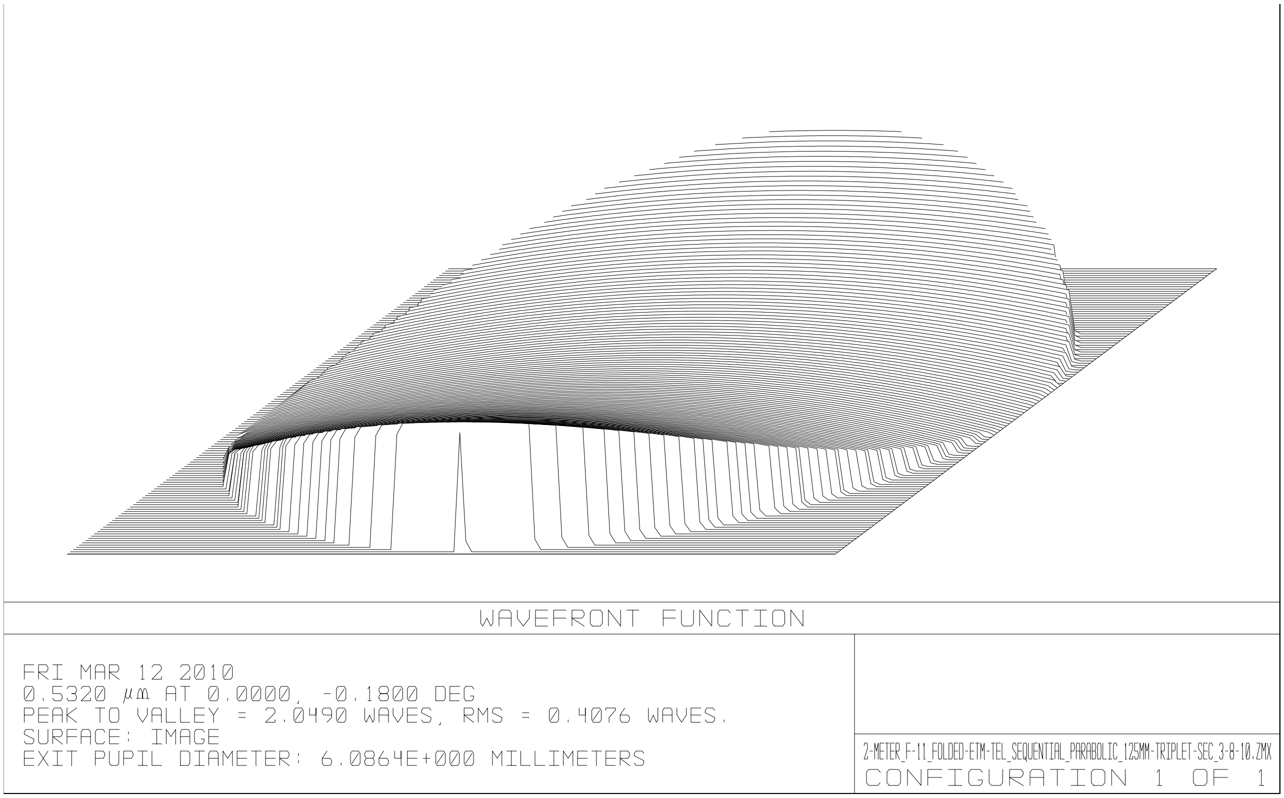

Figure 36: Wavefront Aberration Hartmann Beam, for Parabolic Mirror Primary with 125mm EFL Triplet Lens Secondary

4.5 Summary

The telescope performance for the Hartmann reference beam is summarized below.

Table 5: Ellipticity and Aberration of Hartmann Ref. Beam

Telescope	**Ellipticity**	**Aberration, waves peak to valley**
Off-axis Parabolic	1.017	0.4879
Hybrid, with 4.3 deg incidence spherical secondary	1.59	0.800
Hybrid, with 150mm EFL Triplet Lens Secondary	2.9	4.10
Hybrid, with 125mm EFL Triplet Lens Secondary	3.4	2.05